ELSEVIER

Journal of Structural Geology 27 (2005) 1445–1468

JOURNAL OF STRUCTURAL GEOLOGY

www.elsevier.com/locate/jsg

Microstructural evidence for N–S shortening in the Mount Isa Inlier (NW Queensland, Australia): the preservation of early W–E-trending foliations in porphyroblasts revealed by independent 3D measurement techniques

Mohammad Sayab*

School of Earth Sciences, James Cook University, Townsville QLD 4811, Australia

Received 15 May 2004; received in revised form 11 January 2005; accepted 17 January 2005
Available online 11 July 2005

Abstract

3D microstructural analyses of porphyroblast inclusion trails using both the 'asymmetry switch' method for determining foliation intersection axes preserved in porphyroblasts (FIAs) and the recently developed 'FitPitch' method, reveal W–E- and N–S-trending FIA sets in the White Blow Formation of the Mount Isa Inlier. Each method reveals two subsets of FIAs centered on each of these major trends. These were distinguished based on the relative timing, trend, and orientation of inclusion trail patterns. Thirty-six samples were analyzed using both techniques and produced very similar results. Pitches of the inclusion trails preserved within the porphyroblasts in vertically oriented thin-sections and trends in horizontal sections yield distinct near-orthogonal modal orientations from all the analyzed samples. This indicates that the porphyroblasts host successive fabrics as crenulation foliations and did not rotate with respect to geographical axes. W–E- and N–S-trending FIAs have been obtained from both garnet and staurolite porphyroblasts hosting differentiated crenulation cleavages. Garnet and staurolite growth during bulk north–south shortening recorded the development of multiple foliations and an associated succession of metamorphic events at middle-amphibolite facies conditions that predates the metamorphic history generally recognized in this terrain. This period of bulk shortening and associated metamorphism formed during a period of orogenesis called O_1. W–E shortening formed N–S striking foliations that preserve a period of orogenesis (O_2), and another succession of metamorphism involving more phases of porphyroblast growth preserving N–S-trending FIAs. Overprinting of successive FIA trends (WSW–ENE, WNW–ESE, NNW–SSE, and SSW–NNE) suggests a relative clockwise rotation of the bulk shortening direction through time as it switches from N–S to W–E overall, with a major 'tectonic break' or decompression between O_1 and O_2. The porphyroblast inclusion trail patterns preserving W–E-trending FIAs provide a window into the lengthy period of earlier deformation and metamorphism that is no longer preserved within the matrix foliations.

Keywords: Mount Isa; Eastern Fold Belt; Porphyroblasts; Inclusion trails; Foliation intersection axes

1. Introduction

A development in tectonics has been the recognition of several distinctly oriented successions of datable foliations preserved in porphyroblasts (Bell and Welch, 2002; Williams and Jercinovic, 2002) that potentially allow the reconstruction of the history of the tectonic evolution of large regions (e.g. Bell et al., 2004). This implies the extensive recycling of matrix foliations with deformation and time, but with their preservation in porphyroblasts, allowing them to be used for kinematic analysis (e.g. Steinhardt, 1989; Johnson, 1999; Ilg and Karlstrom, 2000). Studies using porphyroblast inclusion trails across orogenic belts have revealed a prolonged and 'step-by-step' tectonic evolution of multiply deformed terrains (cf. Johnson, 1990a, b and Rosenfeld, 1968; Turnbull, 1981; Thompson and Bard, 1982; Craw, 1985; Aerden, 1998; Bell et al., 1998). Thus, previous studies suggest that only very limited information on tectonics can be gained from macro- and/or mesoscopic scale structures alone because of the strong tendency for progressive shearing to be accommodated along the bedding (e.g. Ham and Bell, 2004).

The Mesoproterozoic Mount Isa Inlier of NW

* Present address: National Centre of Excellence in Geology, University of Peshawar, NWFP, Pakistan
E-mail address: mohammad.sayab@jcu.edu.au.

0191-8141/$ - see front matter © 2005 Elsevier Ltd. All rights reserved.
doi:10.1016/j.jsg.2005.01.013

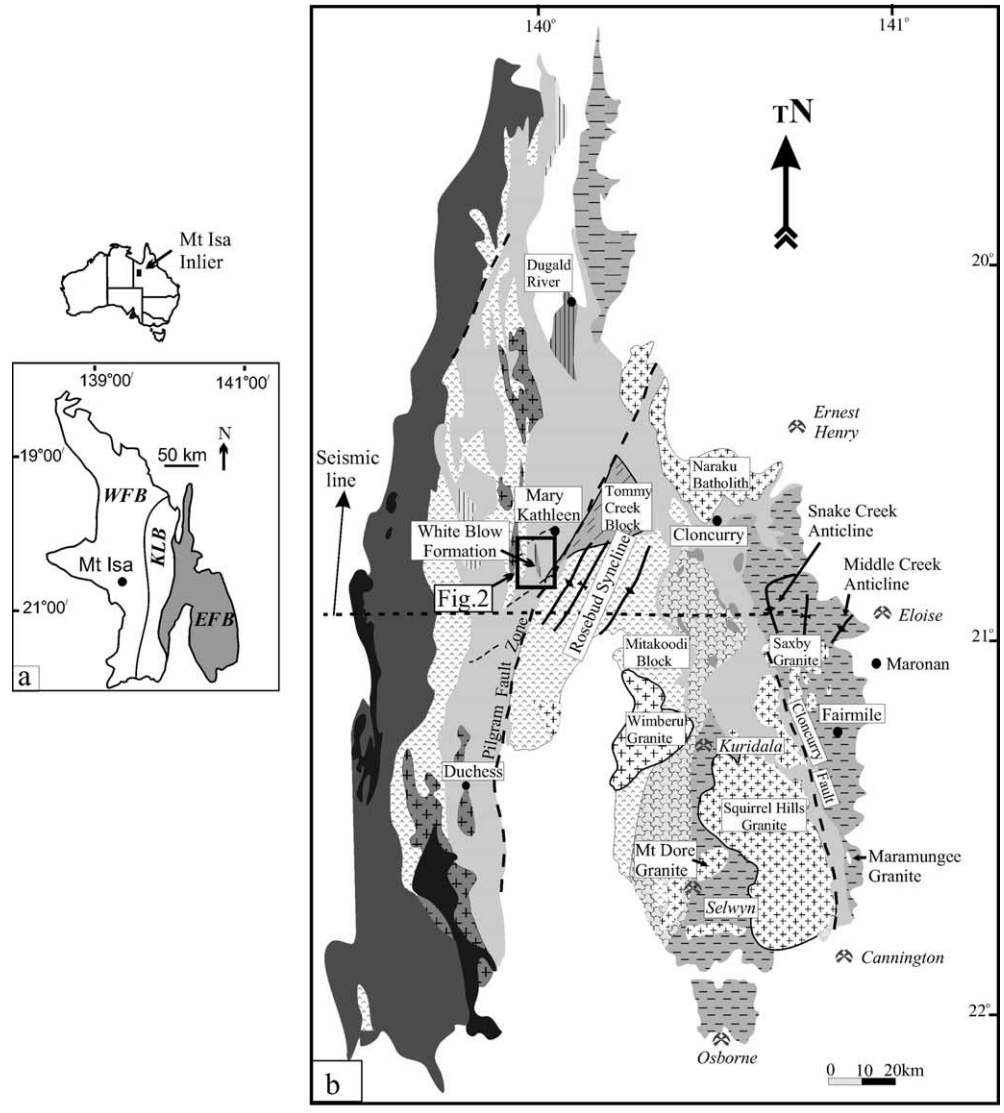

Stratigraphy

- Granite (Williams Batholith, *ca.* 1550-1500Ma)
- Tommy Creek Block (*ca.* 1625Ma)
- Marimo-Staveley Block
  - *Marimo Slate (1655±4 and 1610±5Ma)*
  - *Answer Slate*
  - *Staveley Formation*
- Soldiers Cap Group (*ca.* 1712-1650Ma)
- Roxmere Quartzite
- Granite (Wonga Batholith, *ca.* 1730-1740Ma)
- Mount Albert Group
- Corella Formation (*ca.* 1750±7Ma)
- Argylla Formation (*ca.* 1770±20Ma)
- Undifferentiated units
- Basement (*ca.* 1850-1860Ma)
- Fault
- Major Folds
- *Mine*

Queensland, Australia, is a multiply deformed terrain and a world-class epigenetic base- and noble-metal province (e.g. Oliver et al., 1998). Several structurally controlled, giant mineral deposits are hosted within the inlier. To understand the genesis of these deposits, it is essential that the tectonic processes and overprinting role of multiple deformation phases are well understood as they directly link to prospect analysis and timing and controls on mineralization. Three dominant N–S striking belts have been recognized based on the tectono stratigraphic setting (Blake, 1987). From east to west, these are the Eastern Fold Belt, Kalkadoon–Leichhardt Belt and Western Fold Belt (Fig. 1). The main structural grain of the inlier involves regional N–S oriented upright D_2 structures that resulted from W–E shortening. The role of D_1 is controversial. Recently, it has been argued that the deformation in the Eastern Fold Belt began with W–E extension during D_1, followed by west-vergent thin-skinned or nappe-style folding during D_2, followed by thick-skinned or upright folding and faulting (e.g. Giles and MacCready, 1997; O'Dea et al., 1997a,b; Goleby et al., 1998; MacCready et al., 1998). This argument is based on the W–E oriented Mount Isa Deep Seismic Profile plus some field examples (e.g. Betts et al., 2000). However, Bell (1983), Loosveld (1989) and Bell et al. (1992) have recognized W–E oriented macroscopic scale structures that resulted from earlier N–S shortening in the western and eastern part of the Mount Isa Inlier. They argued that prior to D_2 there was a period of N–S shortening that formed the D_1 event, rather than extension. The presence and nature of the early D_1 structures have been considered controversial in the Eastern Fold Belt of the Mount Isa Inlier due to the intensity of the overprinting D_2 W–E shortening event.

This study geometrically characterizes an earlier period of north–south shortening in the White Blow Formation of the Mount Isa Inlier. The White Blow Formation is located in the middle of the seismic section line (Fig. 1) (MacCready et al., 1998). It produced W–E-trending structures, which are measured by both the 'asymmetry switch' method for FIA (Hayward, 1990; Bell et al., 1998) and the new 'FitPitch' method (Aerden, 2003). These independent techniques produce similar results from more than 600 spatially oriented thin sections, even though the procedures involved are quite different. This paper compares these two independent techniques for measuring foliations preserved in porphyroblasts using the same set of oriented thin sections. It shows that the combination of both techniques provides a robust method for determining the deformation history and for assessing all aspects of 3D geometry of inclusions trails. Significantly, for Isa orogenesis, the early polyphase (e.g. Bell et al., 1992) N–S period of shortening in the Eastern Fold Belt, documented in this study, was accompanied by a significant period of metamorphism that has previously not been distinguished. This causes considerable problems for the above mentioned extensional tectonic model argument that omits the early N–S shortening event (e.g. MacCready et al., 1998; Betts et al., 2000).

2. Geological setting

The Mount Isa Inlier of northwest Queensland, Australia, contains multiply deformed Mesoproterozoic metasedimentary rocks and extensive intrusive and extrusive igneous complexes. The Isan Orogeny occurred between ca. 1620 and 1510 Ma (Page and Bell, 1986). Supracrustal sequences were deposited during episodic extensional and basin forming periods between ca. 1800 and 1620 Ma (Fig. 1) (Beardsmore et al., 1988; Page and Sun, 1998). The present day structural framework of the Mount Isa Inlier consists of N–S striking, intensely deformed, and moderately to steeply dipping D_2 structures with late strike-slip or reverse faults. The nature and existence of pre- or post-D_2 structures and their tectonic implications have been the subjects of considerable controversy (e.g. Loosveld, 1989; Holcombe et al., 1991; Bell et al., 1992; Connors and Lister, 1995; MacCready et al., 1998; Bell and Hickey, 1998; Betts et al., 2000). Low pressure/high temperature (LP/HT) metamorphism with upper amphibolite facies and anticlockwise *P–T–t* paths have been proposed for the Eastern Fold Belt of the Mount Isa Inlier (e.g. Reinhardt, 1992; Rubenach and Lewthwaite, 2002). It has been suggested that peak metamorphic conditions were broadly synchronous with W–E D_2 shortening (e.g. Rubenach, 1992; Rubenach and Barker, 1998; Rubenach and Lewthwaite, 2002). Yet the cause of the initial LP/HT conditions has not been demonstrated in any of these publications.

The White Blow Formation is located in the Eastern Fold Belt, approximately in the middle of the Mount Isa Inlier and provides a key location for the investigation of the structural history of this world-class mineral province (Figs. 1 and 2). It mainly contains Grt–St–Ms–Bt schist (symbols after Kretz (1983)) and records middle-amphibolite facies conditions (Whitelock, 1989). The White Blow Formation is a part of the Mount Albert Group (Derrick et al., 1977). Its lower contact with the Mary Kathleen Group has been interpreted as high angle thrust fault (Fig. 2) (Loosveld and Shreurs, 1987; Whitelock, 1989) so the exact stratigraphic relationship between the Mount Albert Group and the Mary Kathleen Group is uncertain. However, both record the regional D_2 deformation phase of the Isan orogeny (e.g. Blake, 1987; Loosveld, 1989; Holcombe et al., 1991).

Fig. 1. (a) Outline map of the Mount Isa Inlier showing Western Fold Belt (WFB), Kalkadoon–Leichhardt Belt (KLB) and Eastern Fold Belt (EFB). (b) Regional geological map of the Eastern Fold Belt showing major lithotectonic units and location of the study area (modified after Giles and MacCready (1997) and Marshall and Oliver (2001)). Ages after Page and Sun (1998).

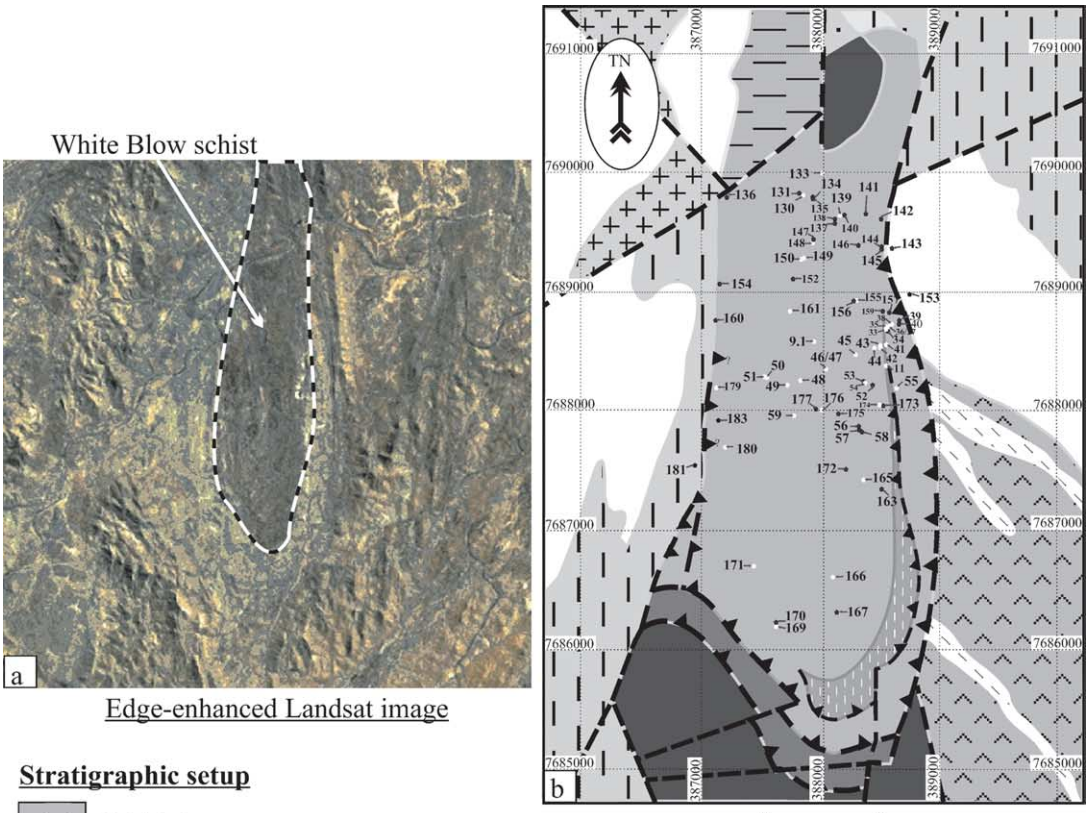

Stratigraphic setup

- Metadolorites
- Graphite-andalusite schist
- Staurolite-garnet schist
- White Blow Fm.
- Deighton Quartzite
- Mt Albert Group
- Calc-silicates
- Green calcareous schists and quartzite
- Grey calcareous schists and quartzites
- Corella Formation
- Mary Kathleen Group
- Baralla quartzite
- Felsic meta-volcanics
- Quartzite
- Argylla Formation

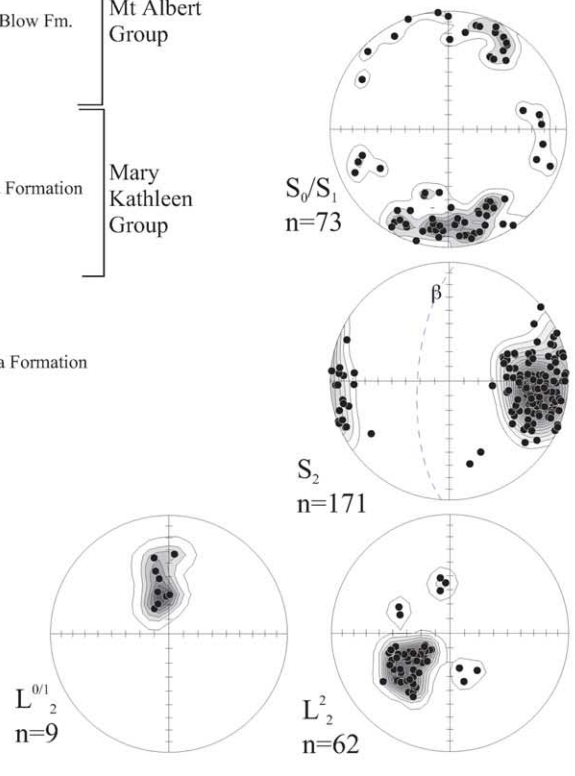

3. Structural field data

S_2 in the Mount Isa Inlier is a steep overall N–S striking foliation, as mentioned above. The geometry of D_1 and associated $S_0//S_1$ in the Eastern Fold Belt are poorly understood, but demonstrably vary with D_2 strain. For example, in high strain areas, $S_0//S_1$ is parallel or sub-parallel to N–S striking S_2, whereas $S_0//S_1$ trends W–E in low strain zones of D_2 (e.g. Loosveld and Shreurs, 1987; Bell et al., 1992; Reinhardt, 1992).

Bedding (S_0) and bedding-parallel foliation (S_1) are well preserved in the White Blow Formation and adjacent Mary Kathleen Group units. In D_2 low strain zones, $S_0//S_1$ dips steeply north or south (Figs. 2c and 3a and b). Where relatively competent west–east striking $S_0//S_1$ structures were observed, S_2 is a crosscutting and spaced foliation, indicating a relatively low influence of the D_2 event on these particular horizons (Fig. 3a and b). Within the White Blow schist, $S_0//S_1$ is largely obscured or transposed due to the dominant pelitic component and high D_2 strain (Fig. 3c). Consequently, the original geometric configuration of S_0/S_1 is difficult to reconstruct. The axial planar D_2 foliation in the White Blow schist is a pervasive, steep to vertically dipping S_2 (Figs. 2c and 3c), associated with a conspicuous steeply southwest plunging mineral lineation L_2^2 (Fig. 3d; terminology after Bell and Duncan, 1978). L_2^2 is mainly defined by biotite in schists and/or amphiboles in calc-silicate rocks. The steeply pitching nature of L_2^2 on S_2 reveals a vertical stretch during the inferred horizontal shortening (see also Reinhardt, 1992). The poles to S_2 produce tight clusters mainly on the eastern half of a Schmidt projection, with the mean S_2 plane oriented almost exactly north–south (Fig. 2c). S_2 in the schist is commonly a differentiated foliation with rare relics of $L_2^{0/1}$ (intersection of S_0/S_1 with S_2) crenulation hinges (Fig. 2c).

4. Sample description

Sixty-five oriented porphyroblastic samples were collected (Fig. 2b). Thirty-seven samples contained inclusion trail patterns of sufficient quality for further microstructural analysis, 30 from the White Blow schist and seven from garnet-bearing calc-silicates. Garnet porphyroblasts are generally small (<0.2–0.3 cm), whereas staurolite porphyroblasts typically range from 0.5 to 1 cm in size (Fig. 3b and d). The metamorphic assemblage visible in thin-section includes Grt, St, Bt and Ms, with rare And, Sil, Gr, Ilm and very rare Rt. Microstructural data were mainly collected from garnet and staurolite porphyroblasts and matrix foliations. Inclusion trail patterns within the porphyroblasts show different stages of differentiation (Bell and Rubenach, 1983) and range from staircase to slightly to moderately sigmoidal shapes (see below).

5. FIA determination and interpretation

5.1. Asymmetry technique

The technique used to measure the FIAs is described by Hayward (1990) and Bell et al. (1995, 1998, 2004). The method involves observing the switch in the asymmetry of curved inclusion trails, preserved in porphyroblasts, in a series of differently oriented thin sections (Fig. 4a). Initially, six vertical thin sections were cut at every 30° interval from true North. Additional thin sections were cut to constrain the asymmetry switch within 10° ($\pm 5°$; see Fig. 4c). The trend of the FIA is taken as being midway between the two oriented vertical thin sections across which the flip occurs, and can be expressed graphically (Fig. 4c and d). Where both asymmetries are observed equally (both 'S' and 'Z'), but the asymmetry in thin sections to either side are switched, the FIA is considered to lie in the plane of that section. The FIA trends are bi-directional so values between 000 and 180° were assigned for simplicity. To determine uni-directional FIA measurements, FIA plunges can be measured by observing the asymmetry switch in radially dipping thin sections cut with strike perpendicular to the FIA trend (e.g. Bell et al., 1995).

5.2. FIA sets

The discovery of sequentially developed multiple fabrics preserved within porphyroblasts needs the development of a strict nomenclature to separate the foliations of different generations. As described below, two dominant bulk shortening events have been recognized based on FIAs separated by a 'tectonic break'. The foliations are numbered in chronological order with respect to successive W–E-trending FIAs as S_a, S_b, S_c… that formed during bulk N–S shortening orogenesis (O_1) and N–S-trending FIAs as S_A, S_B, S_C… that formed during bulk W–E shortening orogenesis (O_2). The terms O_1 and O_2 are used instead of D_1 and D_2, as both periods of shortening are accompanied by multiple phases of deformation and associated middle-amphibolite facies metamorphism. The two orogenic events are separated by decompression (see below; Sayab, in review).

Altogether, 72 FIA measurements were obtained mainly from garnet and staurolite porphyroblasts (Table 1). Fig. 5a shows a rose plot of the total garnet and staurolite FIA

Fig. 2. (a) Edge enhanced Landsat image of the White Blow Formation and adjacent Marry Kathleen Group units. (b) Geological map of the study area (modified from Whitelock (1989)) showing sample locations. Samples with white dots were utilized for 'asymmetry switch' and 'FitPitch' FIA analysis. The prefix WB (White Blow) is removed for each sample to save space. Grid numbers refer to Australian Map Grid (AMG) zone 54. (c) Lower hemisphere equal-area stereo plots for planar and linear structures in the study area.

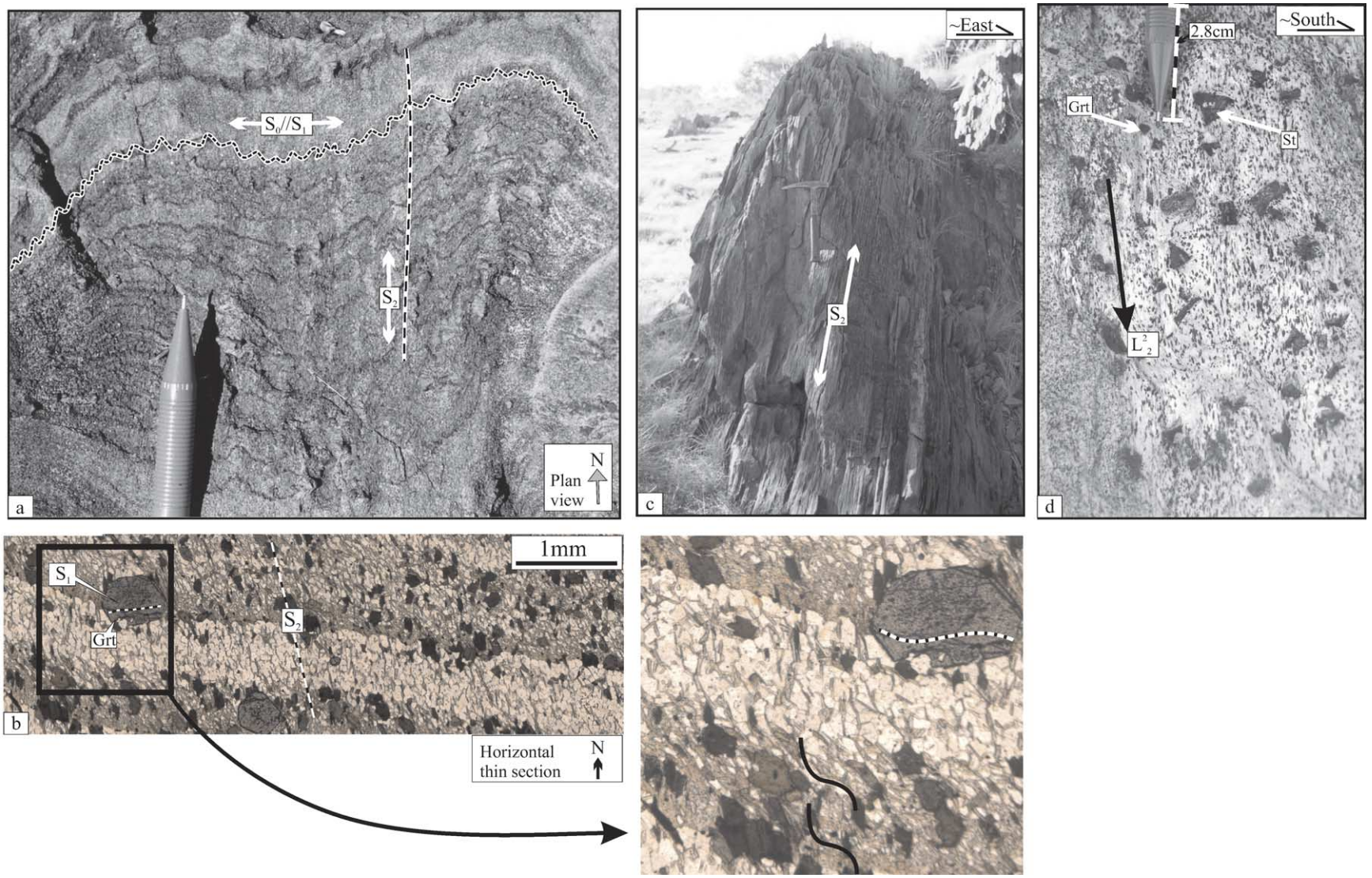

Fig. 3. (a) Spaced S_2 cleavage cross-cutting $S_0//S_1$ in calc-silicates. The garnets are too small (<1.5 mm) to be visible. Length of the pencil in the photograph is 7 cm. (b) Photomicrograph of horizontal oriented thin section showing spaced S_2 cross-cutting $S_0//S_1$. (c) Typical outcrop exposure of the White Blow schist with a pervasive S_2 schistosity. Photograph taken looking north. (d) Grt–St schist (same outcrop as Fig. 3(c)) with steeply southwest plunging L^2_2 Bt mineral lineation. View onto S_2 plane. Abbreviations after Kretz (1983).

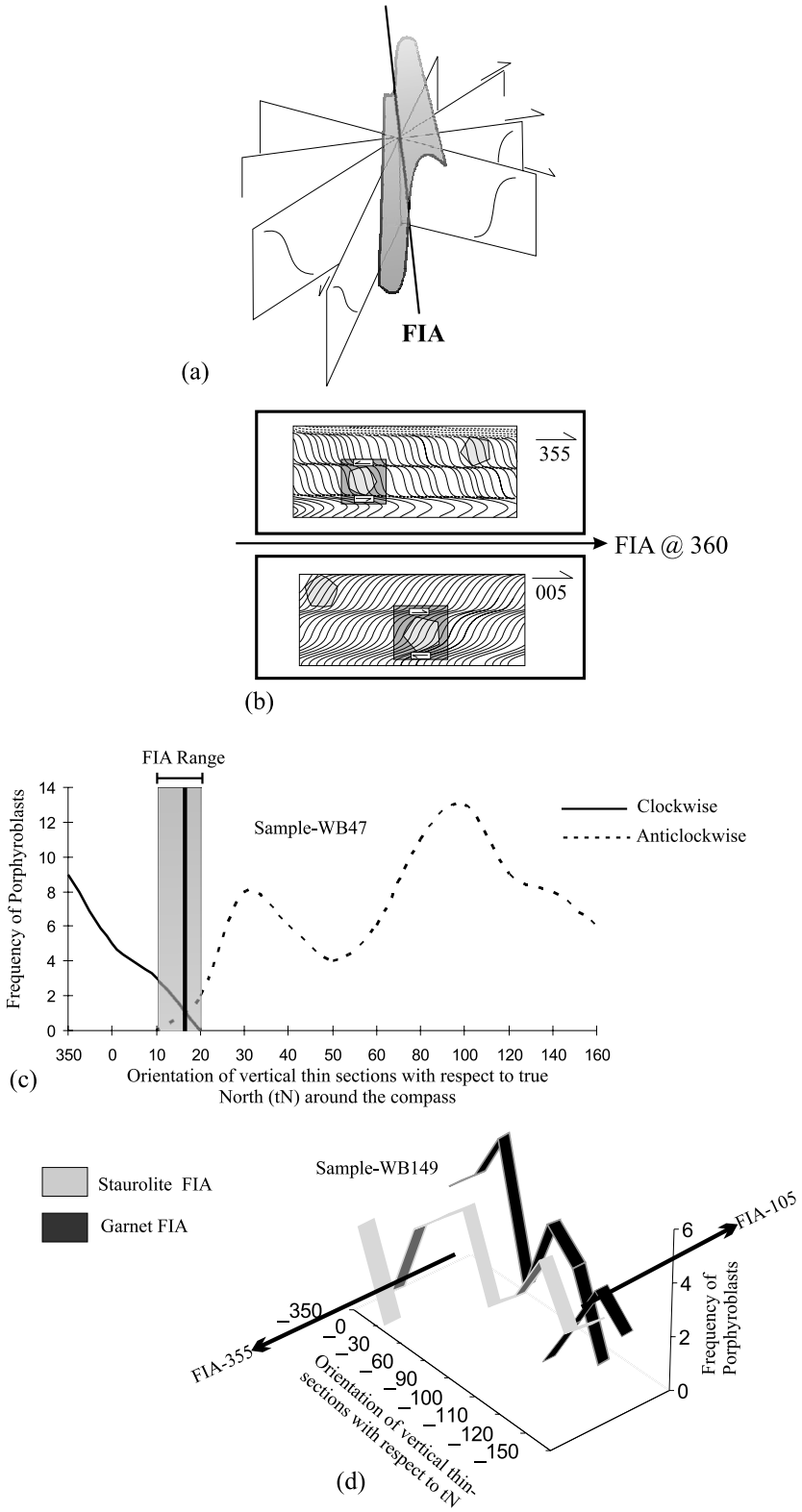

Fig. 4. Diagrams showing method developed by Hayward (1990) and Bell et al. (1995) by which the trends of FIA are measured. (a) Part of an array of vertically oriented thin sections at an acute angle to the fold axis; note switch in the inclusion trail patterns across the axis. If asymmetric microstructures are observed on a fanned array of oriented thin sections maintaining the same viewing direction, then a swap in asymmetry occurs where the axis is crossed. (b) Schematic sketches of vertically oriented thin sections with sigmoidal inclusion trail geometry. In this case, FIA lies between these two thin sections at 000°. (c) An example of how FIA and FIA range are determined graphically. The FIA trend (dark line) corresponds to the crossover, or switch in asymmetries. The FIA range (light gray band) is defined by the interval in which both asymmetries are present. (d) Graphical representation of multi-FIAs for Grt core and St rim in single sample (WB149).

Table 1
Sample locations with respect to Australian Map Grid (AMG) coordinates, the FIA trend measured in them, FIA sets based on their relative timings and 'FitPitch' FIA trend/plunge (symbols after Kretz (1983))

S. No.	Easting	Northing	FIA trend (true North)				Mtx	FIA 1		FIA 2		FIA 3		FIA 4			FitPitch FIA	
			Grt		St													
			Core	Rim	Core	Rim		Grt	St	Grt	St	Grt	St	Grt	St	Mtx		
WB47	388100	7688410		15		15								15	15		13	
WB41	388542	7688637		355	355									355	355		173	
WB38	388604	7688727				5									5		no data	
WB33	388550	7688694		95		10		95							10		98	
WB48	387828	7688263		90	90			90	90								95	9
WB11	388681	7688672	105		105			105	105								112	
WB35	388567	7688718				20									20		25	111
WB149	387854	7689285	105			355	355		105						355	355	293	
WB133	388010	7690005		115	115					115	115						280	
WB176	388003	7688017	115							115							107	
WB171	387434	7686695	115		115					115	115						284	
WB169	387619	7686205	120		120					120	120						288	
WB166	388105	7686616	85	15		15			85					15	15		82	
WB180	387189	7687698	85		85			85	85								85	174
WB179	387118	7688192	100			5			100						5		198	287
WB165	388367	7687426		15		15								15	15		193	
WB155	388294	7688940	150		150									150	150		346	
WB139	388163	7689650			85	120		85			120						81	
WB150	387843	7689284	355		355									355	355		174	
WB161	387739	7688844	85		85	105		85	85		105						82	337
WB148	387934	7689418		0		0								0	0		354	291
WB174	388502	7688059	355											355			351	
WB45	388293	7688477		5		5								5	5		350	
WB49	387712	7688222	85		85			85	85								73	
WB51	387527	7688292	5		100	0			100					5	5		285	
WB50	387537	7688290	105			105		105	105								289	
WB46	388045	7688258	5			5								5	5		352	
WB44	388448	7688532		15		15								15	15		189	
WB42	388600	7688680		5										5			194	
WB36	388570	7688720				105					105						103	
WB9.1	387895	7688562		135		135						135	135				321	
WB37	388600	7688820				355	0								355	0	159	
WB54	388370	7688241		5		20								5	25		192	
WB55	388607	7688217		0		0								0	0		169	
WB59	387772	7687969		95		95		95	95								287	
WB130	387848	7689821	85			85		85	85								80	
WB43	388551	7688563			105	0					105				0		100	354

Mtx: matrix.

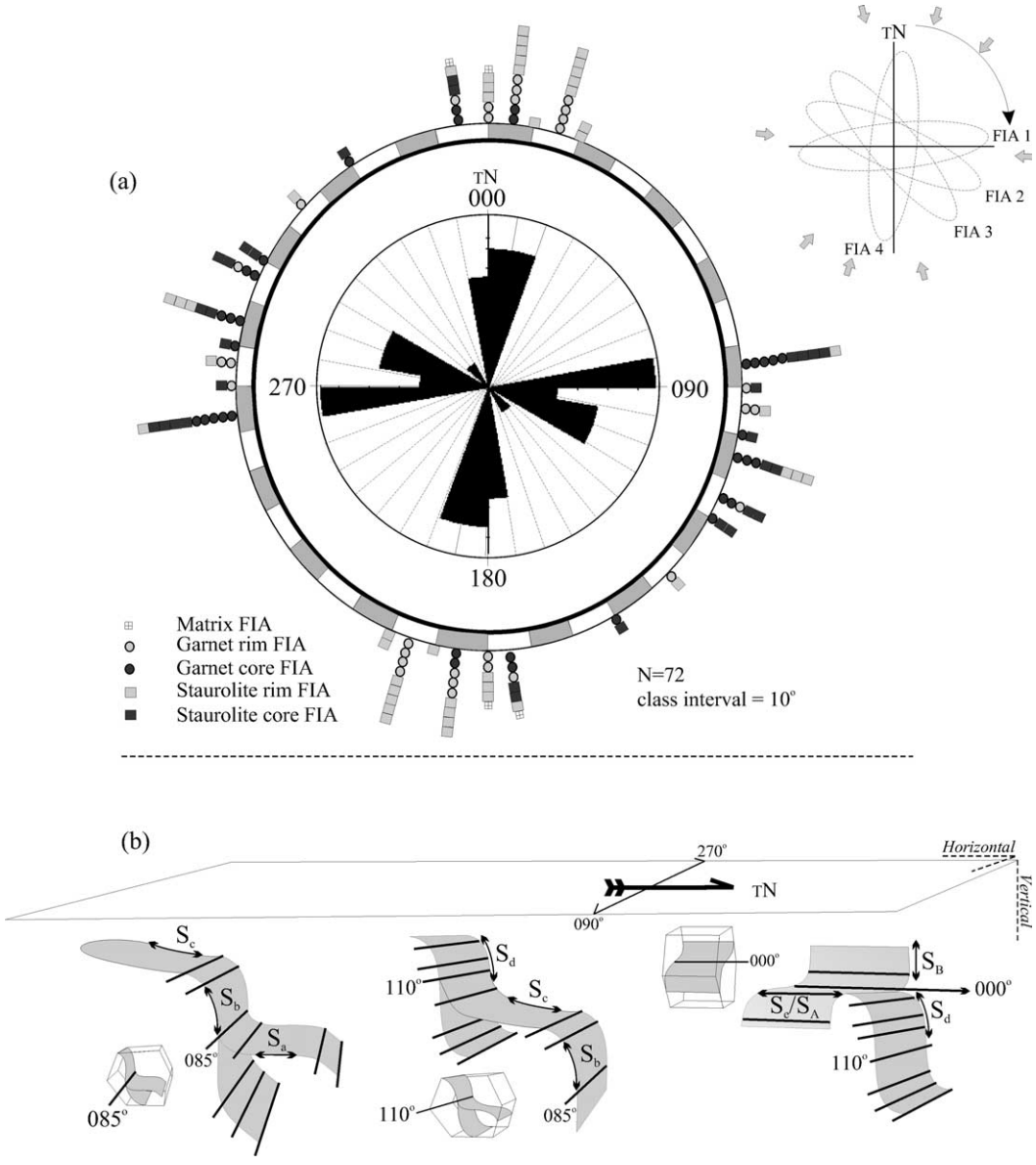

Fig. 5. A rose diagram of FIA trend with respect to true North determined from all Grt and St porphyroblasts. Outer plot gives more details of data for FIA trends from Grt and St porphyroblasts. Note that the WSW–ENE and WNW–ESE FIA trends were mainly obtained from the cores of the porphyroblasts, whereas NNW–SSE and SSW–NNE FIA trends are dominantly obtained from the rims of the individual porphyroblasts. (b) 3D conceptual model showing near-orthogonal multiple deformation history during O_1 and O_2 events of the Isan Orogeny deduced from detailed FIA analysis. Two distinct FIA sets can be recognized during O_1 event of the Isan Orogeny based not only on the FIA trends but also on the geometry of inclusion trail patterns. O_2 produced N–S FIA trend.

trends measured from all samples. Both garnet and staurolite porphyroblasts preserve the dominant W–E and N–S FIA trends. Four separate FIA trends can be seen oriented WSW–ENE, WNW–ESE, NNW–SSE, and SSW–NNE. The last of these, the SSW–NNE FIA trend, parallels the present day structural grain of the White Blow Formation (cf. Fig. 2). FIA sets can be distinguished not only based on the switch of the inclusion trail patterns from clockwise to anticlockwise asymmetries, but also with respect to the change in orientation from subhorizontal to subvertical or vice versa. These relationships are summarized in Fig. 5b. However, the presence of differentiated crenulation cleavage in the porphyroblasts that is not preserved in the matrix reveals that these structures were progressively destroyed by younger events (Figs. 6 and 7).

6. Relative timing of FIAs

FIA sets were recognized based on the relative timing of successive foliations whereby, (1) multi FIA analysis, that is FIAs change trend in a consistent manner from porphyroblast cores to rims in some samples, shown graphically (Fig. 4d; Bell et al., 1998, 2004), (2) successions of prograde

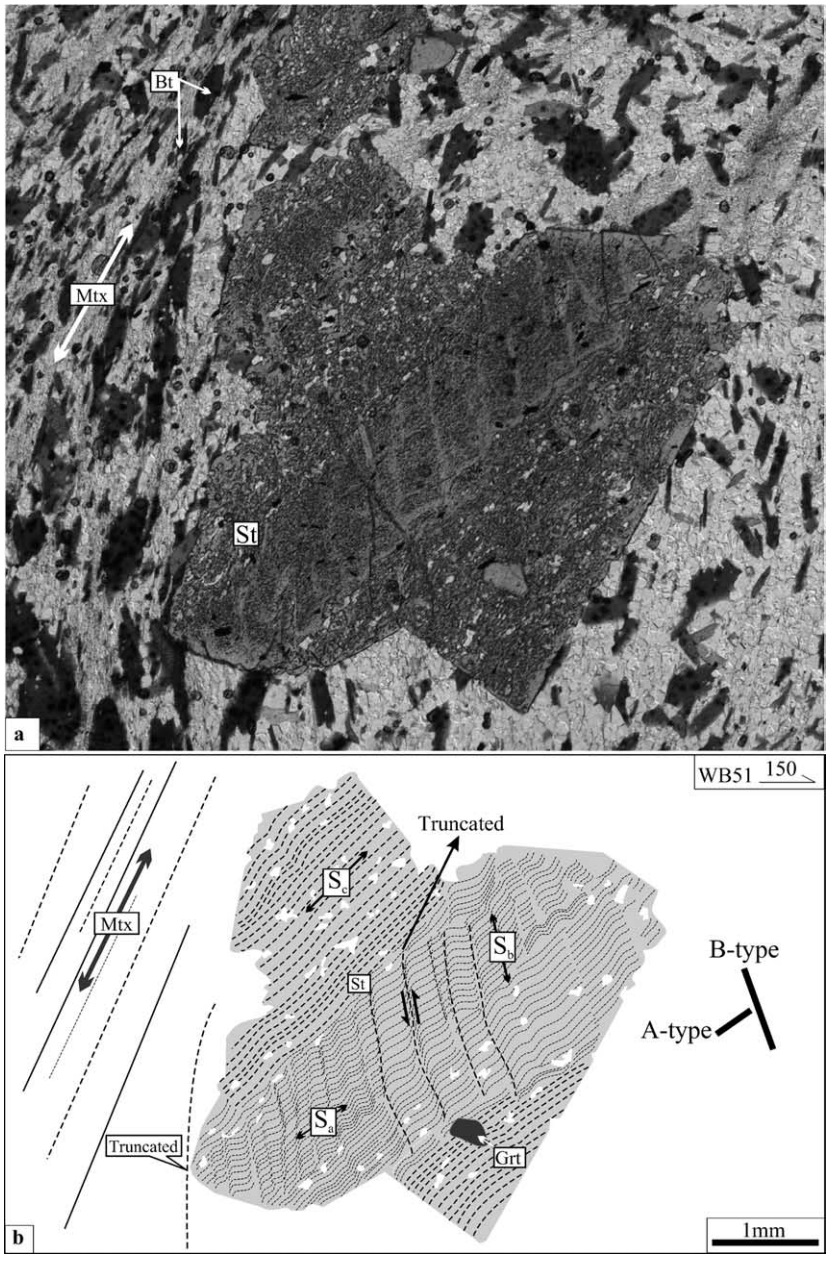

Fig. 6. Photomicrograph of a St porphyroblast hosting stage 3 differentiated crenulation cleavage in the core. The asymmetry associated with the cleavage is anticlockwise and have a 100° FIA trend (set 1). At the rim of the porphyroblast, shallow pitching S_c is overprinted. For 'FitPitch' analysis, the microstructures have been divided into 'A' and 'B' type (see text for discussion).

porphyroblast growth hosting different orientations or generations of inclusion trails, for example garnet inside staurolite, (3) truncation vs. continuous inclusion trail microstructures (e.g. Adshead-Bell and Bell, 1999), and (4) FIA trends near-parallel or perpendicular to outcrop foliation.

6.1. FIA set 1

A few multi FIA samples have been recognized from garnet and staurolite porphyroblasts (Table 1). Garnet and/or staurolite porphyroblasts containing the 080–105° FIA range of trends dominantly contain subhorizontal inclusion trails in the core that curve to subvertical at the median and/or rim with clockwise or anticlockwise asymmetries (Fig. 6). Inflection and/or truncation of the subvertical or steep inclusion trails to subhorizontal at the rims are uncommon in garnet porphyroblasts, but common in the staurolite (Fig. 6). The inclusion trails in porphyroblasts preserving these FIA orientations are at stage 3–4 of differentiated crenulation cleavage development (Bell and Rubenach, 1983) and are not continuous with the matrix foliation. The nomenclature of the inclusion trail foliations preserved within the porphyroblasts hosting this FIA population has been allocated based on relative timing of

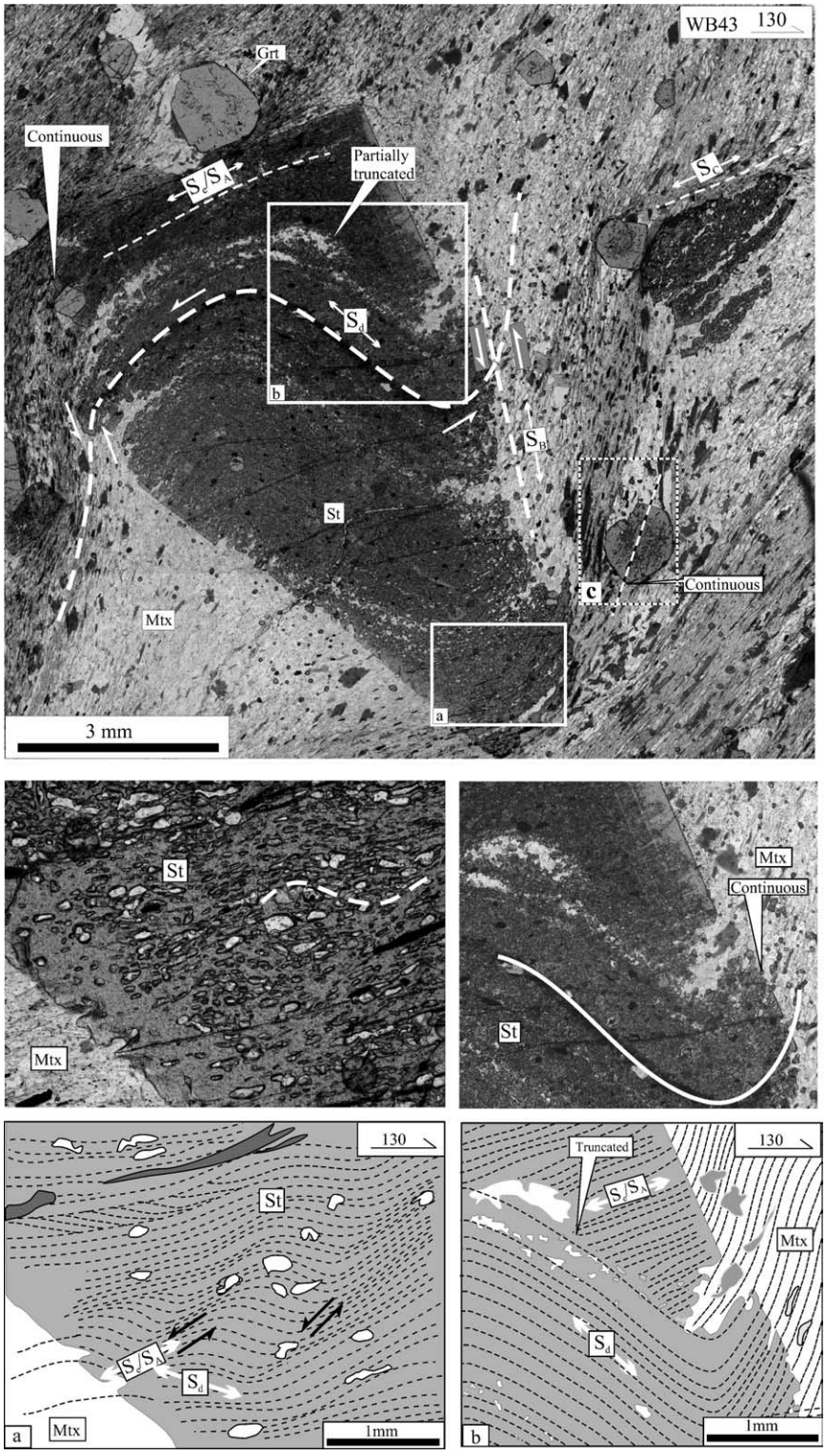

Fig. 7. An example of subidioblastic St porphyroblast showing sigmoidal inclusion trail geometry. (a) At high magnification, it was observed that the porphyroblast preserved differentiation rather than simple sigmoidal inclusion trail patterns. Anticlockwise asymmetry can be observed along differentiated seams preserved within the porphyroblast. The porphyroblast hosts deformation fabric elements, which are steeply to moderately pitching S_d to shallow pitching S_e/S_A and steeply pitching S_B. (b) S_d is partially truncated with S_e/S_A at the median region, whereas S_B is continuous with the matrix. (c) Grt porphyroblast preserves straight steep S_B and are continuous with the matrix.

crenulated versus crenulation cleavages. Porphyroblasts preserving subhorizontal foliation S_a were followed by steep axial planar S_b and then subhorizontal S_c (Fig. 6).

6.2. FIA set 2

Garnet and staurolite porphyroblasts preserve 105–120°-trending FIAs belong to set 2. The inclusion trail geometries are dominated by moderately dipping or subvertical patterns in the core curving to subhorizontal orientations at the rim (Fig. 7). However, at high magnification (~20–30×), subhorizontal crenulations can be observed within the steep inclusions trails. FIA set 2 occurs in garnet and staurolite porphyroblasts hosting subhorizontal S_c, which was the end product of FIA set 1, followed by steep S_d and then subhorizontal S_e (Figs. 5b, 6 and 7). The steep foliation (S_d) preserved within the porphyroblast controls the trend (105–120°) of FIA set 2. Fig. 7 shows a subidioblastic staurolite porphyroblast hosting a deformation sequence from S_d to S_e and $S_e(S_A)$ to S_B. It is noticeable that the inclusion trails within the core of the porphyroblast show partial truncational patterns that is between S_d and S_e/S_A.

Two samples preserve both the FIA set 1 and FIA set 2 from the core to rim, respectively, of the porphyroblasts (samples WB161 and WB139). None of these porphyroblasts have inclusion trails continuous with the matrix foliation. Thus, several samples preserve a consistent geometric succession from flat to steep to flat about one FIA trend in one set of garnet porphyroblasts (FIA 1), followed by flat to steep and then flat for the second FIA trend for the other set (FIA 2; 5b).

6.3. FIA set 3

Sample WB9.1 contains a 135° FIA resulting from a transition from subhorizontal to subvertical inclusion trails at the rim of the porphyroblasts. Therefore, it can be inferred that the rock preserves shallow S_e curving into a moderately steep foliation at the rim S_f that controls the FIA trend (135°). This FIA trend was only obtained from one rock sample (WB9.1).

6.4. FIA set 4

A fourth set of samples with porphyroblasts containing FIA ranging between 350 and 020° have moderate to subhorizontal inclusion trails in the core and subvertical trails in the rim. Roughly 60% of these foliations preserved as inclusion trails are continuous with the matrix foliations, especially those where the FIA ranges between 000 and 020° (Figs. 7 and 8). Those with FIA trends ranging between 350 and 000° are mostly truncated. This fourth FIA set results from W–E shortening (the O_2 event) of subhorizontal S_A in the core or rim (Figs. 7 and 8) that curves into and is continuous with the matrix S_B foliation. The subhorizontal S_A of O_2 appears to be equivalent to the subhorizontal S_e of O_1.

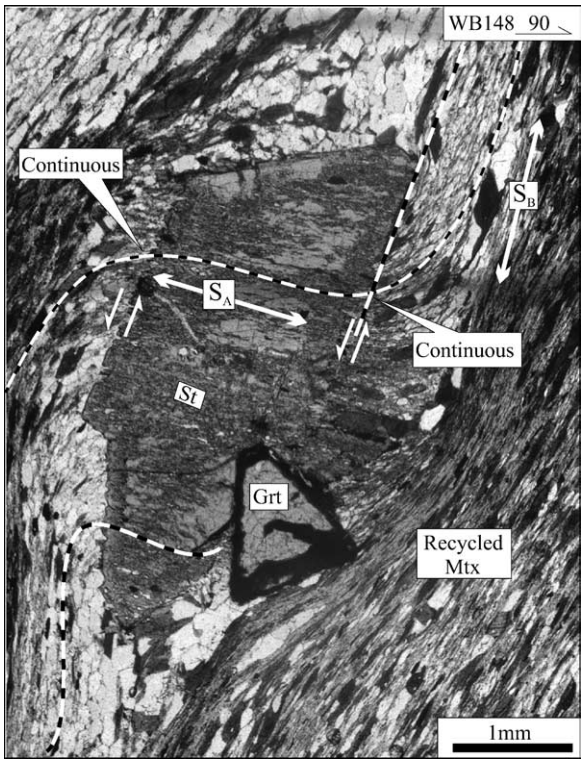

Fig. 8. Excellent example of continuous inclusion trail microstructures. 000–020° FIAs (set 4) have been obtained from all those Grt and St porphyroblasts, which are continuous with the matrix foliation.

7. Matrix microstructures and correlation with field structures

The matrix foliation is a product of extensive recycling of foliations through repeated reactivation and reuse of earlier foliations (e.g. Ham and Bell, 2004). However, in low strain zones or relatively competent portions of the rock, overprinting relationships can be preserved and correlated with the orientation of inclusion trails within the porphyroblasts. For example, several N–S vertically oriented thin-sections from the White Blow schist contain subvertical S_b and/or S_d foliation overprinted by subhorizontal S_c and/or S_e semi-differentiated crenulations (Fig. 9). This geometric relationship is evident from those porphyroblasts showing FIA 1 and 2 from subhorizontal to subvertical inclusion trail patterns or vice versa. In the W–E oriented thin sections, both garnet and staurolite preserve shallow $S_e(S_A)$ that is continuous with the matrix S_B (Fig. 8), which is the dominant foliation of the White Blow Formation. Therefore, the N–S striking S_2 in the field is actually the S_B of O_2.

8. 'FitPitch' technique

Measurements of particular planar structures as apparent dips on different sections around the compass should lie in a plane when plotted on a stereographic projection. Therefore,

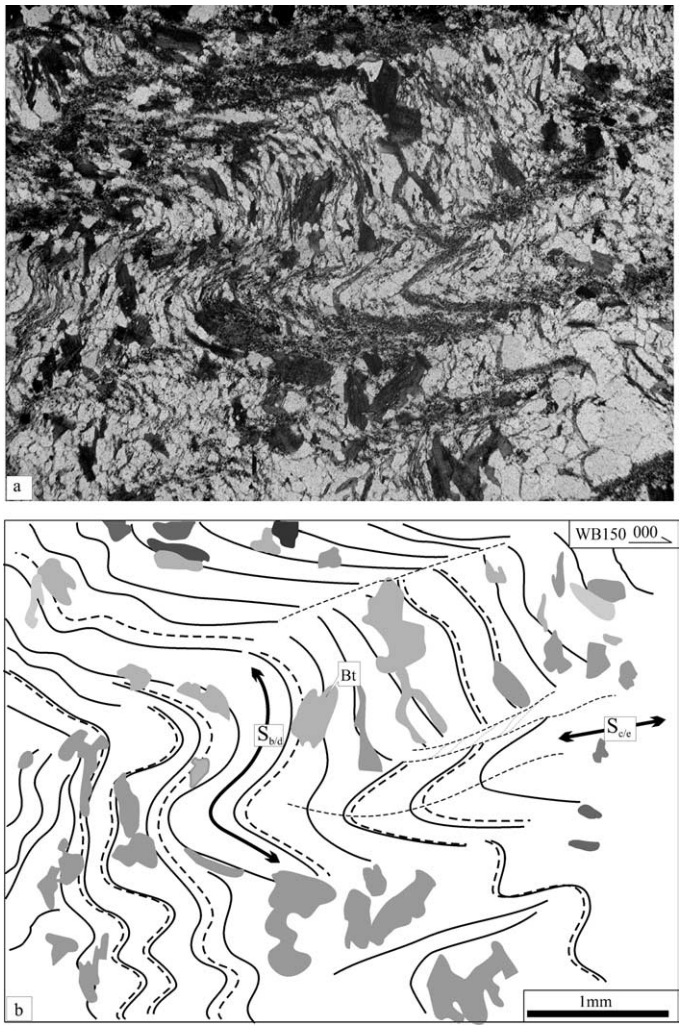

Fig. 9. Photomicrograph and associated line diagram of vertical N–S striking thin section showing tight to isoclinal folds with subhorizontal S_c or S_e axial planar trace in the matrix. The rock sample is from low strain zone of S_2.

several measurements of one generation of inclusion trail pitches from a radial set of vertical oriented thin sections can be used to estimate and construct the foliation plane defined by those inclusion trails. This approach has been applied using a recently developed computer program called 'FitPitch', which calculates one, two or three best-fit planes based on uni-, bi- or trimodal groups of linear structural elements distributed in 3D-space with statistical constraints (Aerden, 2003). The intersection of the two best-fit planes from two distinct orientations of pitches should, theoretically, define the FIA (Aerden, 2003). 'FitPitch' is especially useful for those inclusion trail patterns showing no asymmetry or close to straight orientations. FIA set(s) can potentially be determined using 'FitPitch' for foliations that show no asymmetric curvature. Such foliations cannot be used to measure FIAs by the 'asymmetry switch' method. Another advantage of the 'FitPitch' technique is that the program calculates the FIA plunge and trend based on the intersection of two best-fit planes (Aerden, 2003) as discussed below.

8.1. Measuring procedures

Seven oriented thin sections, six of which are vertical at 30° intervals around the compass and one of which is horizontal, were prepared from each sample for 3D-microstructural analysis using the 'FitPitch' computer program. Thirty-six samples were analyzed. One sample (WB38) was not suitable for recording pitches because of the complex geometry of the inclusion trails. The same vertical oriented sets of thin sections were used for the conventional FIA method. An additional horizontal thin section was prepared for each sample to constrain the strike of the inclusion trails (Aerden, 2003).

Data were divided into two main groups (after Aerden, 2003). A-type microstructures were classified as straight to moderately sigmoidal inclusion trails and B-type microstructures were classified as axial traces of microfolds or different stages of differentiated crenulation cleavages (Fig. 6) (Bell and Rubenach, 1983). A total of 3835 pitches were measured both from A- and B-type microstructures preserved within the porphyroblasts and plotted on rose

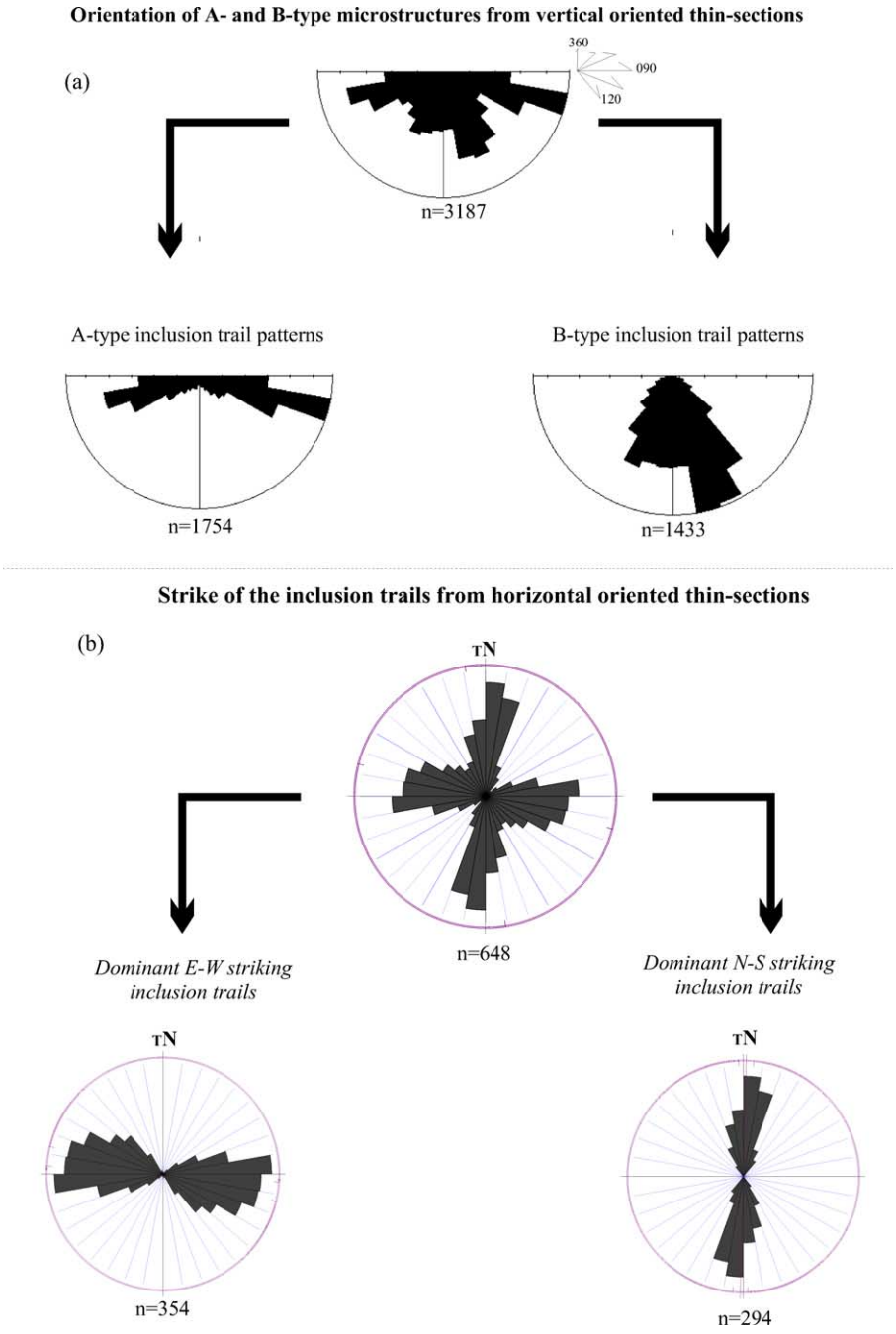

Fig. 10. Rose diagrams showing pitches of the inclusion trails measured from oriented thin sections. (a) Inclusion trail pitches showing distinct subhorizontal A-type and subvertical B-type modes from vertical oriented thin sections. (b) Rose diagrams showing two dominants strike orientations recorded from horizontal oriented thin sections from all the analyzed rocks for 'FitPitch'. Note that the number of W–E oriented inclusion trail pitches are dominantly preserved within the porphyroblasts (see also Fig. 3b).

diagrams (Fig. 10). A distinct gently dipping modal peak was obtained for A-type microstructures and a steeply dipping modal peak for B-type microstructures (Fig. 10a). Horizontal thin sections show dominantly W–E and N–S strikes of inclusion trails in the porphyroblasts (Fig. 10b). Data from individual thin sections have been plotted on the rose diagrams and exhibit bi- or trimodal inclusion trail pitches. Data were not recorded from the low density inclusion trail patterns that locally occur at the rim of the porphyroblasts or from poorly defined patterns.

8.2. Results

Most of the 36 analyzed samples yield similar results (Fig. 11a) to that obtained using the conventional or 'asymmetry switch' FIA method. Table 1 shows a comparison

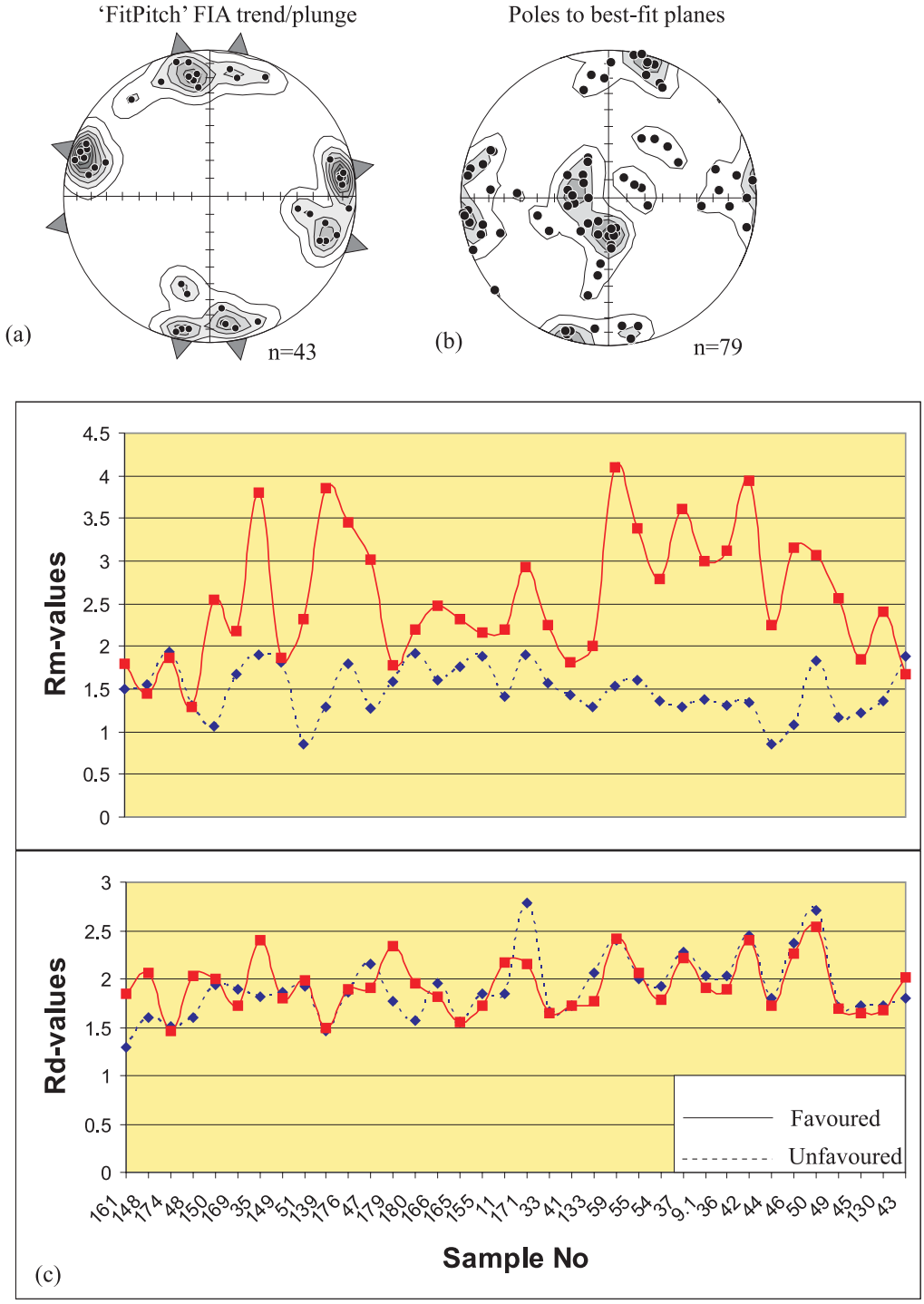

Fig. 11. (a) Lower-hemisphere equal-area stereographic plot showing FIA trend and plunge calculated by 'FitPitch'. (b) Poles to the best-fit planes calculated by 'FitPitch'. Note that the poles are preferentially located at the periphery and near center of the stereo plot (see text for discussion). (c) Graph showing quantitative 'FitPitch' R_d and R_m values from all the analyzed samples (samples along x-axis without prefix WB). Two plane R_d/R versus three plane R_d/R_m values are plotted. The selection of a two- or three-plane solution is based on the highest R_d and R_m values and textural relationships. Note that the R_d values are almost equal. However, R_m values are significantly higher and preferred for each and every sample.

of 'FitPitch' with the conventional FIA method. The 'FitPitch' method produced two significant advantages. FIA trends were obtained from inclusion trail patterns with no asymmetry. For example, W–E FIA trends were obtained from samples WB48 and WB180 using both the techniques (Table 1). However, 'FitPitch' calculates additional N–S FIA from inclusion trails preserved within the porphyroblasts that show no asymmetry and are continuous with the matrix foliation (Fig. 7c; Table 1). These N–S FIA trends are in excellent agreement with those samples that do show inclusion trail asymmetry. Similarly,

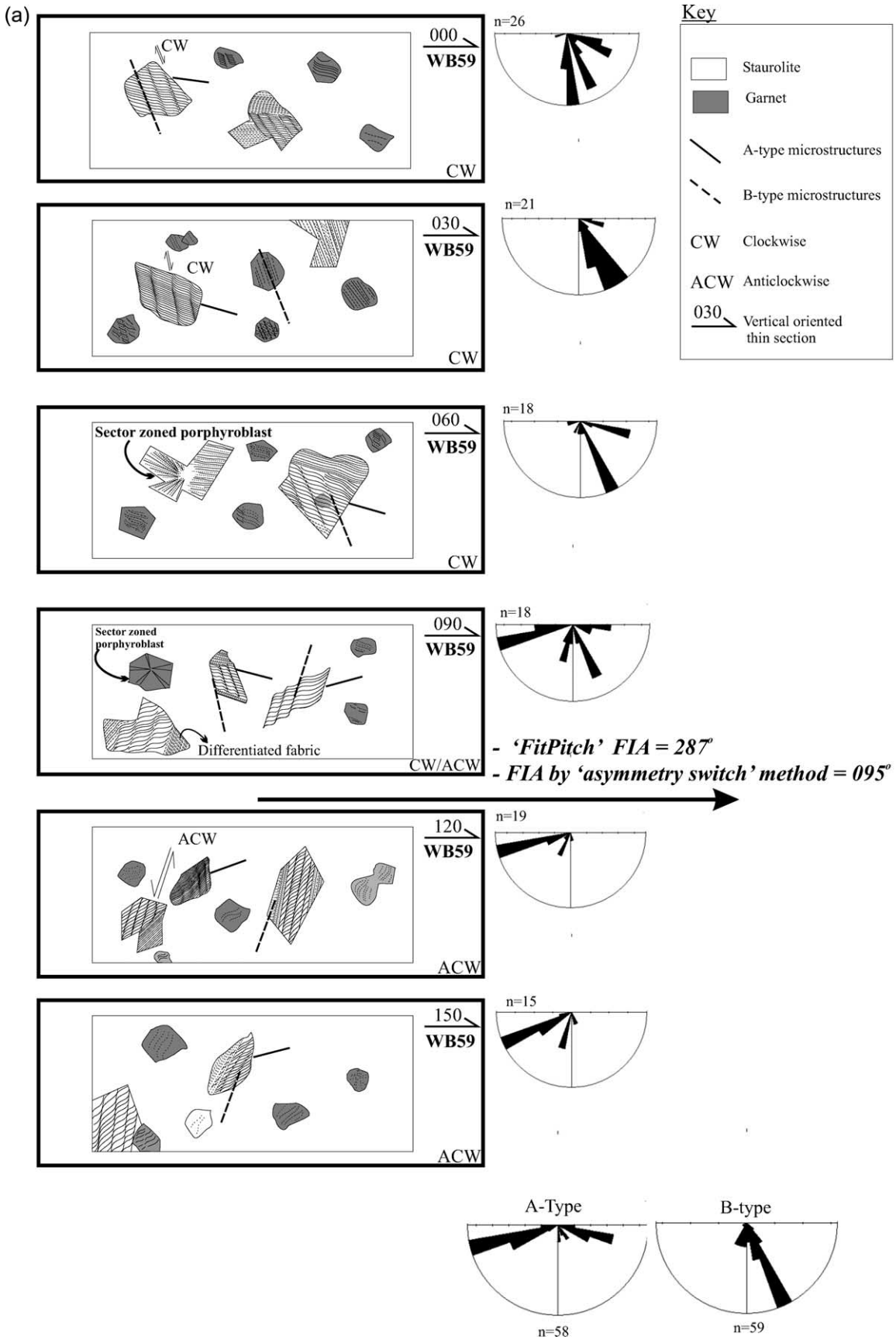

Fig. 12 (*Caption on next page*).

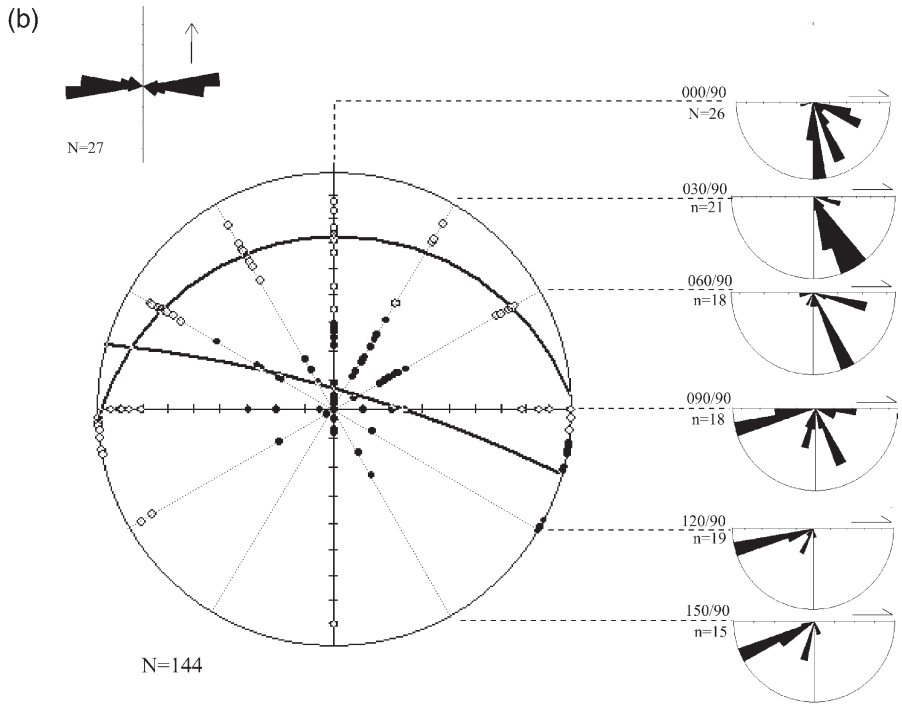

Best Poles	Rd	Rm	FIA
196/07; 177/62	2.516	4.097	287/11 (2-plane) - favoured
227/20; 126/04;177/64	2.502	1.531	027/69; 325/22; 035/21 (3-plane) - unfavoured

Fig. 12. (a) Sketches showing an example of how FIA can be determined by 'asymmetry switch' and 'FitPitch' techniques. 095° FIA was obtained using the 'asymmetry switch' method for this specimen (WB59) as 080° and 090° azimuth thin sections contain porphyroblasts with dominant clockwise, whereas 100° azimuth thin section contains porphyroblasts with dominant anticlockwise asymmetries. 'FitPitch' calculates 287/11 degree FIA trend and plunge. If data from two additional thin sections are added, e.g. 080° and 100°, 'FitPitch' FIAs would lie very close to the 'asymmetry switch' method. (b) Stereographic plot showing two-plane solution with 287/11 FIA trend and plunge for sample WB59 with high R_d and R_m value. The two-plane solution is in excellent agreement with microstructural constraints (cf. Fig. 12a).

'FitPitch' calculates an additional W–E FIA trend for samples WB35 and WB148 that were not determined by the 'asymmetry switch' method.

In addition, 'FitPitch' calculates the FIA plunge (Fig. 11a). It is noticeable that almost all the FIA plunges lie at less than 40°. Similarly, poles to the best-fit planes are preferentially located at the periphery and near the center of the stereo plot (Fig. 11b), further strengthening the data shown in Fig. 10 with optimal statistical constraints (Fig. 11c). Fig. 12a and b are excellent examples of how 'FitPitch' calculates FIA based on a two best-fit plane solution with high R_d and R_m values (see below).

8.3. Criteria for choosing 'FitPitch' two- or three-bestfit planes: textural vs. statistical constraints

The advantage of data acquisition through the conventional FIA method is that it not only constrains the geometry of inclusion trail patterns, but also the relative timing of porphyroblast growth with respect to multiple foliation development. Measuring pitches for 'FitPitch' and correlating microstructures with known and unknown timing with respect to porphyroblast growth and foliation development need strict criteria. Interpretation of this data has a strong influence on best-fit planes and their respective FIAs using the 'FitPitch' program. For example, 'FitPitch' can calculate two closely-spaced steeply dipping best-fit planes with favorable statistical calculations and a FIA trend and plunge. However, it will be shown here that it might be possible that those two closely-spaced steeply oriented best-fit planes are, indeed, one steep plane based on textural relationships, even though statistically this may not be favored. That is, FIA from two steep planes may be just an artifact (see also Aerden (2003)).

Aerden (2003) proposed that data should be fitted to one, two or three best-fit planes, whichever produces the smallest standard deviation for high R_d and R_m values. R_d is expressed as the degree of the tightness of the best-fit plane solution, whereas R_m is the degree of internal consistency of a data set from radial thin sections. During data collection it was observed that inclusion trails for one generation, or related to one deformation event, always have slightly different orientation from porphyroblast to porphyroblast and from thin section to thin section. This occurs because of: (1) variation in the amount of rotation of the foliation by synchronous deformation prior to porphyroblasts growth during a single deformation phase (Fig. 13a); (2) anastomosing cleavages included at different porphyroblast growth sites (Fig. 13b); (3) a cut effect.

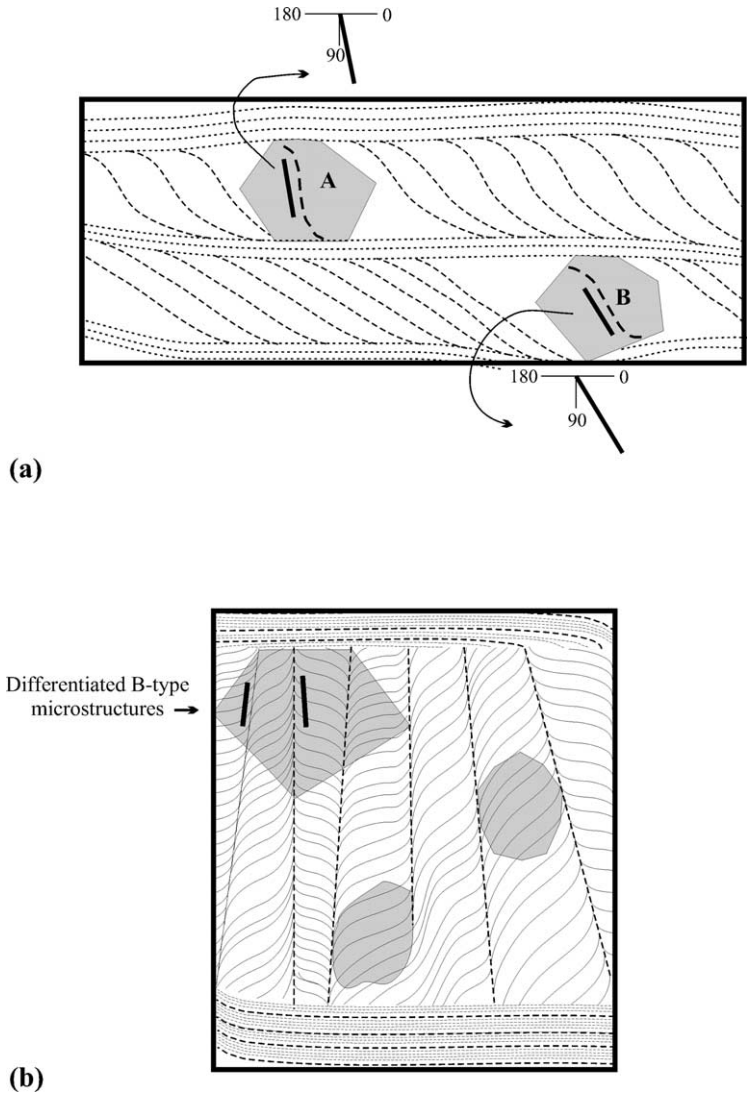

Fig. 13. (a) Sketch showing two slightly differently oriented inclusion trail pitches preserved within the porphyroblasts belonging to one generation in one thin section. Data with varying orientation from different oriented thin sections around the azimuth may fall into the two-plane solution with best statistical constraints for inclusions trails belonging to one deformation. (b) Differentiated B-type microstructures with opposite dips related to one deformation event (see text for further discussion).

Therefore, data from moderately varying inclusion trails from six different oriented vertical thin sections may statistically fall into two best-fit plane solutions rather than one plane. Nevertheless, the two-planes with tight statistical constraints would lie close to each other and actually result from one plane (Fig. 14). Similarly, a three plane best-fit solution yields three FIAs, which may be statistically favored, but may not be in agreement with textural relationships. The extra FIA(s) are just an artifact. In this study, most of the samples analyzed by 'FitPitch' are in good agreement both texturally and statistically with respect to two- or three-plane solutions (Figs. 10 and 11).

8.4. Samples with three-plane solution

Most of the samples calculated with a three-plane solution show porphyroblasts with an extended microstructural history, e.g. steep S_d in the core followed by gently dipping $S_e(S_A)$ in the median and steep S_B in the rim, which is in most cases continuous with the matrix foliation (Fig. 7). However, not all the porphyroblasts show an extended microstructural history and few multi FIAs have been obtained. W–E or N–S FIAs were obtained using the conventional FIA method except for samples WB33, WB149, WB166, WB179, WB51, and WB43 (Table 1). Multi FIAs were also obtained using 'FitPitch' for samples WB48, WB35, WB180, WB179, WB161, WB148, and WB43. Inclusion trails from porphyroblasts showing no asymmetry yield N–S (samples WB48, WB161, and WB180) or W–E (samples WB148 and WB35) FIAs in a three-plane solution. For example, in sample WB43 (Fig. 15a), a 105° FIA was obtained by the conventional FIA method from S_d to S_e, whereas a 000° FIA was obtained for

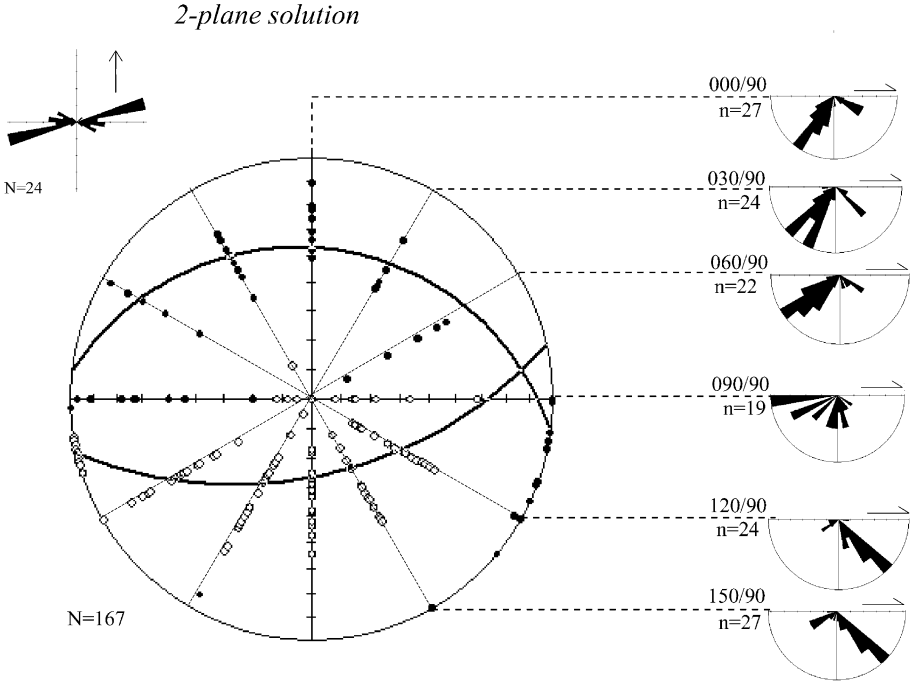

Sample No. WB166			
Best Poles	**Rd**	**Rm**	**FIA**
187/53; 347/26	1.813	2.481	82/11 (2-plane) - favoured
188/51; 346/34; 336/06	1.917	1.596	84/11; 69/22; 244/17 (3-plane) - unfavoured

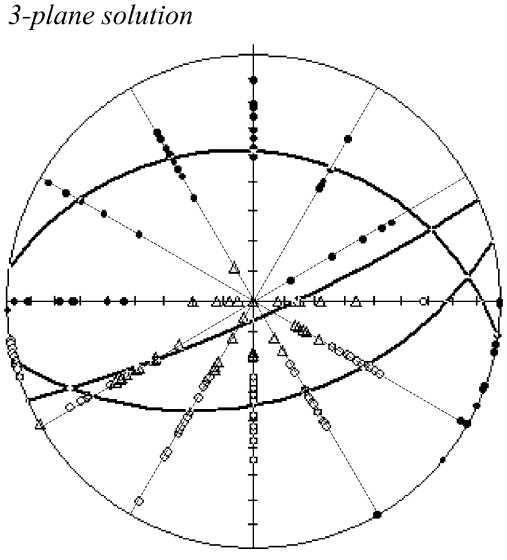

Fig. 14. Lower-hemisphere equal-area stereo plot with two- and three-plane solutions and rose diagrams from vertical oriented thin sections (WB166). The two-plane solution is favored as it is more consistent with the microstructures (cf. with rose plots). Note that the 'FitPitch' divided one steep plane into two with high R_d and low R_m values with three FIAs and is not preferred based on the microstructural relationships. The third FIA is an artifact.

$S_e(S_A)$ to S_B. Porphyroblasts preserving only S_B and showing no asymmetry also yields N–S FIA. This relationship is consistent with respect to the orientation of pitches of the inclusion trails and, therefore, a three-plane solution is in agreement with both statistical constraints and the textural relationships.

9. Discussion and conclusions

9.1. 'Asymmetry switch' technique vs. 'FitPitch'

Both techniques give similar results from the same set of oriented thin sections, even though the procedures are quite

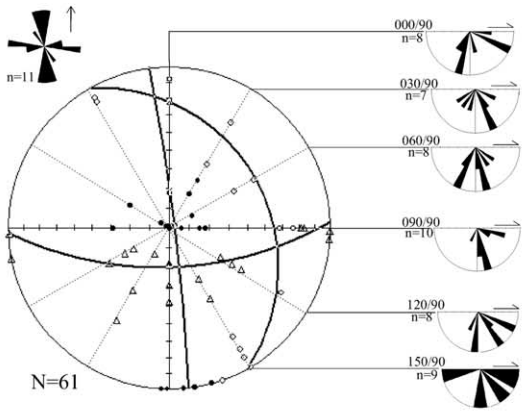

Sample No. WB43			
Best Poles	**Rd**	**Rm**	**FIA**
255/29; 356/12	1.697	1.976	105/75 (2-plane) - unfavoured
263/02; 241/52; 358/20	2.011	1.711	354/17; 166/70; 100/31 (3-plane) - favoured

(a)

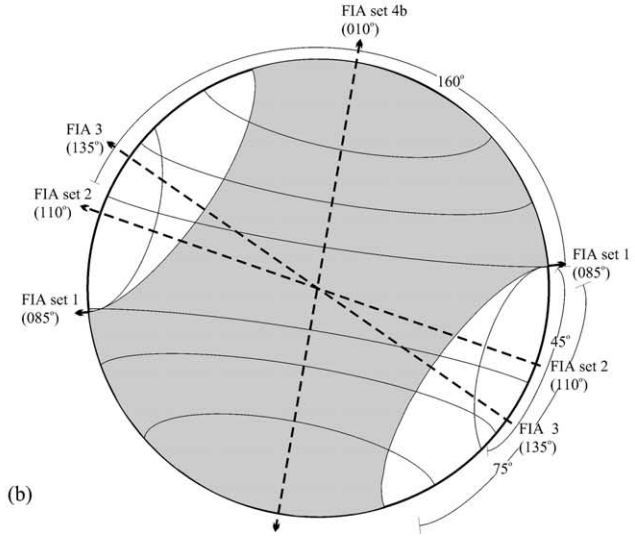

Fig. 15. (a) Sample WB43. Three-plane solution with steep S_d, shallow S_e and steep S_B with 100/31 and 354/17 FIA trend/plunge, respectively. 166/70 FIA trend/plunge is an artifact as explained in the text. The three-plane solution is in good agreement microstructurally and statistically. (b) Stereo plot showing the effects of rotating FIA set 1 around the mean trend of the next FIA in the succession. Effects of rotating FIA set 1 around the mean trend of FIA set 2 by 100°, recorded by FIA set 2, spreads FIA set 1 trends over at least 45°. Effects of further rotating FIA set 1 around FIA 3 spreads FIA set 1 trend over at least 75°. Effects of rotating FIA set 1 around FIA set 4 produced spread of FIA set 1 over at least 160°.

different. This strong agreement confirms the validity of both methods for determining the FIA trends preserved within the porphyroblasts. In particular, the early formed W–E oriented structures related to O_1 have been thoroughly documented in spite of the fact that they are no longer preserved within the matrix. 'FitPitch' generates very close ($\pm 5°$) FIA trend/plunge results to the 'asymmetry switch' method, if 18 equally spaced vertical oriented thin section are analyzed, but this is more costly and time-consuming (cf. Fig. 12a). The 'asymmetry switch' method is extremely useful in determining the timing of porphyroblast growth with respect to foliation development and determining shear senses across the regional folds or pre-existing folds (e.g. Ham and Bell, 2004). However, this method cannot be used for porphyroblasts with straight inclusion trails and

additional differently dipping thin sections striking perpendicular to the FIA trend are needed to find the FIA plunge.

The invention of 'FitPitch' provides a method that uses different criteria than the 'asymmetry switch' method to characterize the orientation of FIAs with statistical constraints. The program complements the existing asymmetry technique and is useful as an alternative to assess the different generations of FIAs determined by the Hayward (1990) method. 'FitPitch' not only calculates FIA trends but also FIA plunges without the need for the extra differently dipping thin sections. However, without reliable textural relationships, this technique is not useful for timing the FIA with respect to foliation development and porphyroblast growth. The combination of both techniques provides a powerful and robust method for determining the deformation history and for assessing all aspects of 3D geometry of inclusion trails.

The program could potentially be improved, as 'FitPitch' cannot distinguish textural relationships that statistically favor either two- or three-plane solutions, as discussed above. This can be solved by adding nomenclature, if possible, to the data file to specify microstructures. For example, if nomenclature is assigned to steep differentiated cleavages of one generation preserved in porphyroblasts, then 'FitPitch' will not divide the result into two steep planes (cf. Fig. 14). This would influence the interpretation of timing of differently oriented planes on a stereo plot.

9.2. Implications of FIA sets for Isan Orogenesis

In a group of recent publications (e.g. Goleby et al., 1998; MacCready et al., 1998; Betts, et al., 2000) it has been argued that deformation in the Eastern Fold Belt of the Mount Isa Inlier involved thin-skinned non-coaxial deformation followed by thick-skinned deformation based on the W–E oriented Mount Isa Deep Seismic Profile. An interesting aspect of this seismic study is that most of the structures are interpreted as kilometer scale nappe-folds, whereas, the surface geology is characterized by a steep fabric along the transect (e.g. Australian Bureau of Mineral Resources 1:100,000 scale maps and cross-sections). Indeed, 3D gravity and magnetic geophysical data in the form of 'geophysical worms-multiscale-edge analysis' indicate steep lithological boundaries and, consequently, steep structures deep within the crust consistent with the outcrop-scale geology (Predictive Mineral Discovery, Cooperative Research Center, internal data). This makes interpretation of the seismic section ambiguous. Moreover, Bell et al. (1992) recognized multiple subvertical and subhorizontal foliations and associated stretching lineations that developed during a N–S shortening event in the Wonga–Duchess Belt and Rosebud Syncline lying adjacent to the study area (Fig. 1). This data is strongly supported by the evidence for multiple generations of foliations that produced the N–S O_1 shortening described herein, which predate the matrix foliation preserved in these rocks.

3D-microstructural analysis has revealed the existence of early formed foliations as crenulation cleavages preserved within the porphyroblasts. The first formed shallowly plunging 080–105° oriented FIA set defined by shallow S_a in the core, differentiated steep S_b, and shallow S_c at the rim of the porphyroblasts, indicate a primary phase of N–S shortening. S_b formed as the axial plane foliation to F_1 folds with W–E oriented fold axes during O_1. The second FIA set, which lies between 105 and 120°, resulted from steep S_d overprinted by shallow S_e and indicates a second period of bulk shortening. The third FIA at 135° observed only in one rock sample, preserving shallow S_e curving into a moderately steep S_f, suggests a gradual transition from N–S O_1 shortening to W–E O_2 shortening or the waning stages of the overall N–S shortening phase of the Isan Orogeny. It appears that subhorizontal S_e remained the dominant foliation at the end of O_1 rather than S_f and defines the decompression phase of the O_1 orogenesis (Sayab, in review).

O_2, the product of W–E bulk shortening, is preserved throughout the entire Eastern Fold Belt by N–S pervasive fabrics in the matrix that have been previously called S_2 in the field (e.g. Betts et al., 2000). This phase of orogenesis obliterated and obscured previously formed structures in the inlier. Porphyroblast growth hosting shallow $S_A(S_e)$ with inflection due to S_B at the rim continued during the deformation and metamorphism that accompanied O_2. Most porphyroblasts hosting shallow S_A in the core and steep S_B in the rim have FIAs lying between 350 and 000° and are generally not continuous with the matrix. On the other hand, FIAs lying between 000 and 020° have inclusion trails that are continuous with the matrix and resulted from the last stage of porphyroblast growth. This slight variation from 350 to 000° and 000 to 020° suggests a slight change in bulk shortening direction. This study complements Mares (1998), who found early W–E followed by N–S FIAs in the Fairmile area of the Eastern Fold Belt (Fig. 1).

9.3. Correlating multiple phases of metamorphism based on FIA sets

It is generally assumed that porphyroblast growth is broadly synchronous with syn-metamorphic-tectonic processes in a homogenous matrix (e.g. Kohn et al., 1992; Florence et al., 1993; Vance and Mahar, 1998). In these studies, most of the aspects of garnet nucleation and growth have been covered, without putting or classifying them into different tectonic modes with respect to foliation development. However, in a group of recent studies, based on a very detailed microstructural work, it has been demonstrated that porphyroblast growth is episodic and heterogeneously developed from sample to sample (e.g. Aerden, 1998; Bell and Welch, 2002). Therefore, constructing *P–T* paths from just a few samples and inferring tectonic processes without absolute or relative timing constraints on porphyroblast growth with respect to multiple foliation development is

meaningless. The acquisition of more meaningful *P–T* estimates requires detailed microstructural analysis or, more specifically, FIA analysis in the first instance to establish the timing of porphyroblast growth with respect to bulk shortening. For instance, 9-component MnNCKFMASH pseudosections were prepared from garnet bearing schists (Grt–Ms–Bt–And schist) from the Snake Creek Anticline of the Eastern Fold Belt. Garnet in these samples contains N–S and W–E FIAs. Garnet porphyroblasts preserving early W–E FIAs have relatively higher-pressure cores (5–6 kb) than those hosting N–S FIAs (2.5–4 kb). These results are consistent with early N–S shortening and associated medium pressure conditions followed by decompression (with the production of And/Crd) at the end of O_1. Garnet cores preserving N–S FIAs began to grow during LP/HT conditions with increasing pressure during W–E shortening or 'O_2' (Sayab, in review). This study shows the pre-eminence of 3D-FIA analysis not only in determining deformation phases with respect to foliation development, but also in revealing early phases of porphyroblast growth and metamorphism that accompanied N–S shortening during O_1. This also explains the earlier phase of metamorphism O_1 followed by decompression (subhorizontal Se at the end of O_1) responsible for LP/HT conditions in the Mount Isa Inlier, which was not previously recognized from any part of the Mount Isa Inlier (cf. Pattison et al., 1999; Rubenach and Lewthwaite, 2002).

9.4. Implications of FIA for porphyroblast non-rotation versus rotation

Both porphyroblast rotation (e.g. Regnier et al., 2003) and non-rotation models (e.g. Bell et al., 2004) are still used as kinematic indicators to unravel the structural histories of the orogenic belts. The rotational model is generally described as involving non-coaxial shear within a shear zone (e.g. Williams and Jiang, 1999), whereas the non-rotational model involves multiple generations of crenulation cleavage development and associated episodic porphyroblast growth irrespective of whether there is shearing (Bell and Johnson, 1989). Significantly, rotational models have only been applied to porphyroblasts containing spiral trails or sigmoidal patterns (e.g. Rosenfeld, 1968; Passchier et al., 1992) on one-thin section per rock without comprehensive 3D-analysis of inclusion trails. Non-rotational models provide an explanation for the geometries of inclusion trail patterns from spiral to staircase end members and from differentiated crenulations to reactivated fabric in the porphyroblasts (e.g. Bell et al., 2004).

Most of the porphyroblasts in this study preserved differentiated crenulations and/or staircase or sigmoidal geometries. No arguments against staircase inclusion patterns or porphyroblast showing differentiated crenulation cleavages have appeared in the literature so far (e.g. figs. 7.4 and 7.5 of Passchier and Trouw, 1998). Additionally, FIA analysis with distinct model azimuths with respect to geographical reference axes, using either the 'asymmetry switch' or the 'FitPitch' method, provides considerable data demonstrating that porphyroblasts retain original foliations as crenulation cleavages and can be linked to deformation phases that are no longer preserved in the matrix. Pitches of the inclusion trails preserved within the porphyroblasts measured from oriented thin sections indicate near-orthogonal patterns; that is, early W–E followed by younger N–S trends in horizontal thin sections and shallow and steep modes in vertical thin sections, respectively. These results are similar to early W–E and younger N–S FIAs. If the porphyroblasts were rotated, then the pitches on the rose diagrams should be all over the place. Moreover, if rotation of the porphyroblasts had occurred within the matrix during progressive deformation, an enormous spread of FIA trends would have developed. If FIA set 1 was rotated about the axis of FIA set 2, FIA set 3 and FIA set 4 (Fig. 15b; see also Ham and Bell, 2004) an enormous spread of FIA set 1 around the compass would have resulted. Similarly, spreads would have developed in FIA sets 2 and 3. This is not the case and the FIA sets are tightly constrained. Therefore, the porphyroblasts did not rotate during successive deformation events.

Acknowledgements

This work is funded through an International Post-graduate Research Scholarship (IPRS), James Cook University Post-graduate award and *pmd**CRC top-up scholarship to MS. The author gratefully acknowledges Dr M. Rubenach, Prof. T. Bell and Dr A. Ham for fruitful discussion on FIAs. Constructive journal reviews were made by Prof. Laurel Goodwin and Prof. Domingo Aerden. Many thanks to Prof. Joao Hippertt for final review and editorial handling.

References

Adshead-Bell, N.S., Bell, T.H., 1999. The progressive development of a macroscopic upright fold pair during five near-orthogonal foliation-producing events: complex microstructures versus a simple macro-structure. Tectonophysics 306, 121–147.

Aerden, D.G.A.M., 1998. Tectonic evolution of the Montagne Noire and possible orogenic model for syn-collisional exhumation of deep rocks, Hercynian belt, France. Tectonics 17, 62 (see also p. 79).

Aerden, D.G.A.M., 2003. Preferred orientation of planar microstructures determined via statistical best-fit of measured intersection-lines: the 'FitPitch' computer program. Journal of Structural Geology 25, 923–934.

Beardsmore, T.J., Newbery, S.P., Laing, W.P., 1988. The Maronan supergroup: an inferred early volcanosedimentary rift sequence in the Mount Isa Inlier, and its implications for ensialic rifting in the middle Proterozoic of northwest Queensland. Precambrian Research 40 (41), 487–507.

Bell, T.H., 1983. Thrusting and duplex formation at Mount Isa, Queensland, Australia. Nature 304, 493–497.

Bell, T.H., Duncan, A.C., 1978. A rationalized and unified shorthand terminology for lineation and fold axes in tectonites. Tectonophysics 47, T1–T5.

Bell, T.H., Hickey, K.A., 1998. Multiple deformations with successive subvertical and subhorizontal axial planes in the Mount Isa Region: their impact on geometric development and significance for mineralization and exploration. Economic Geology 93, 1369–1389.

Bell, T.H., Johnson, S.E., 1989. Porphyroblast inclusion trails: the key to orogenesis. Journal of Metamorphic Geology 7, 297–310.

Bell, T.H., Rubenach, M.J., 1983. Sequential porphyroblast growth and crenulation cleavage development during progressive deformation. Tectonophysics 92, 171–194.

Bell, T.H., Welch, P.W., 2002. Prolonged Acadian Orogenesis: revelations from foliation intersection axis (FIA) controlled monazite dating of foliations in porphyroblasts and matrix. American Journal of Science 302, 549–581.

Bell, T.H., Reinhardt, J., Hammond, R.L., 1992. Multiple foliation development during thrusting and synchronous formation of vertical shear zones. Journal of Structural Geology 14, 791–805.

Bell, T.H., Forde, A., Wang, J., 1995. A new indicator of movement direction during orogenesis: measurement technique and application to the Alps. Terra Nova 7, 500–508.

Bell, T.H., Hickey, K.A., Upton, J.G., 1998. Distinguishing and correlating multiple phases of metamorphism across a multiply region using the axes of spiral, staircase and sigmoidal inclusion trails in garnet. Journal of Metamorphic Geology 16, 767–794.

Bell, T.H., Ham, A.P., Kim, H.S., 2004. Partitioning of deformation along an orogen and its effects on porphyroblast growth during orogenesis. Journal of Structural Geology 26, 825–845.

Betts, P.G., Ailleres, L., Giles, D., Hough, M., 2000. Deformation history of the Hampden Synform in the Eastern Fold Belt of the Mt Isa terrane. Australian Journal of Earth Sciences 47, 1113–1125.

Blake, D.H., 1987. Geology of the Mount Isa Inlier and environs, Queensland and Northern Territory. Australian Bureau of Mineral Resources, Geology and Geophysics, Bulletin 225, 1–83.

Connors, K.A., Lister, G.S., 1995. Polyphase deformation in the western Mount Isa Inlier, Australia: episodic or continuous deformation? Journal of Structural Geology 17, 305–328.

Craw, D., 1985. Structure of schist in the Mt. Aspiring region, northwestern Otago, New Zealand. New Zealand Journal of Geology and Geophysics 28, 55–75.

Derrick, G.M., Wilson, I.H., Hill, R.M., Glikson, A.Y., Mitchell, J.E., 1977. Geology of the Mary Kathleen 1:100,000 Sheet area, northwest Queenland. Australia BMR, Geology and Geophysics, Bulletin 193.

Florence, F.P., Spear, F.S., Kohn, M.J., 1993. P–T paths from northwestern New Hampshire: metamorphic evidence for stacking in a thrust/nappe complex. American Journal of Science 293, 939–979.

Giles, D., MacCready, T., 1997. The structural and stratigraphic position of the Soldier Cap Group in the Mount Isa Inlier. In: Ailleres, L., Betts, P. (Eds.), Structural elements of the Eastern Succession—a field guide illustrating the structural geology of the Eastern Mount Isa Terrane, Australia, vol. 63. Australian Crustal Research Centre, Technical Publication, pp. 61–73.

Goleby, B.R., MacCready, T., Drummond, B.J., 1998. The Mount Isa Geodynamic Transect-Crustal Implications. In: Braun, J., Dooley, J., Goleby, B., Van der Hilst, R., Klootwijik, C. (Eds.), Structure and Evolution of the Australian Continent Geodynamic, vol. 26. American Geophysical Union, pp. 109–117.

Ham, A.P., Bell, T.H., 2004. Recycling of foliations during folding. Journal of Structural Geology 26, 1989–2009.

Hayward, N., 1990. Determination of early fold axis orientation in multiply deformed rocks using porphyroblast inclusion trails. Tectonophysics 179, 353–369.

Holcombe, R.J., Pearson, P.J., Oliver, N.H.S., 1991. Geometry of a Middle Proterozoic extensional decollement in northeastern Australia. Tectonophysics 191, 255–274.

Ilg, B.R., Karlstrom, K.E., 2000. Porphyroblast inclusion trail geometries in the Grand Canyon: evidence for non-rotation and rotation? Journal of Structural Geology 22, 231–243.

Johnson, S.E., 1990a. Lack of porphyroblast rotation in the Otago schists, New Zealand: implications for crenulation cleavage development, folding and deformation partitioning. Journal of Metamorphic Geology 8, 13–30.

Johnson, S.E., 1990b. Deformation history of the Otago schists, New Zealand, from progressively developed porphyroblast-matrix micorstructures: uplift-collapse orogenesis and its implications. Journal of Structural Geology 12, 727–746.

Johnson, S.E., 1999. Porphyroblast microstructures: a review of current and future trends. American Mineralogist 84, 1711–1726.

Kohn, M.J., Orange, D.L., Spear, F.S., Rumble, D., Harrison, M.T., 1992. Pressure, temperature and structural evolution of west-central New Hampshire: hot thrusts over cold basement. Journal of Petrology 33, 521–556.

Kretz, R., 1983. Symbols for rock-forming minerals. American Mineralogist 68, 277–279.

Loosveld, R.J.H., 1989. The synchronism of crustal thickening and high T/low P metamorphism in the Mount Isa Inlier, Australia 1. An example, the central Soldiers Cap belt. Tectonophysics 158, 173–190.

Loosveld, R., Shreurs, G., 1987. Discovery of thrust klippen, northwest of Mary Kathleen, Mt Isa Inlier, Australia. Australian Journal of Earth Sciences 34, 387–402.

MacCready, T., Goleby, B.R., Goncharov, A., Drummod, B.J., Lister, G.S., 1998. A framework of overprinting orogens based on interpretation of the Mount Isa deep seismic transect. Economic Geology 93, 1422–1434.

Mares, V.M., 1998. Structural development of the Soldiers Cap Group in the Eastern Fold Belt of the Mt Isa Inlier: a succession of horizontal and vertical deformation events and large-scale shearing. Australian Journal of Earth Sciences 45, 373–387.

Marshall, J.L., Oliver, N.H.S., 2001. Mechanical controls on fluid flow and brecciation in the regional host rocks for Eastern Fold Belt ironstone Cu–Au deposits. Mt Isa Block. Geological Society of Australia, Specialist Group in Economic Geology Mineralisation, alteration and magmatism in the Eastern Fold Belt, Mount Isa Block Australia. Geological Review and Field Guide, Special Publication 5, pp. 30–45.

O' Dea, M.G., Lister, G.S., MacCready, T., Betts, P.G., Oliver, N.H.S., Pound, K.S., Huang, W., Valenta, R.K., 1997a. Geodynamic evolution of the Proterozoic Mount Isa terrane. In: Burg, J.P., Ford, M. (Eds.), Orogeny Through Time, vol. 121. Geological Society of London Special Publication, pp. 99–122.

O' Dea, M.G., Lister, G.S., Betts, P.G., Pound, K.S., 1997b. A shortened intraplate rift system in the Proterozoic Mount Isa terrain, NW Queensland, Australia. Tectonics 16, 425–441.

Oliver, N.H.S., Rubenach, M.J., Valenta, R.K., 1998. Precambrian metamorphism, fluid flow, and metallogeny of Australia. Journal of Australian Geology and Geophysics 17, 31–53.

Page, R.W., Bell, T.H., 1986. Isotopic and structural responses of granite to successive deformation and metamorphism. Journal of Geology 94, 365–379.

Page, R.W., Sun, S.-S., 1998. Aspects of geochronology and crustal evolution in the Eastern Fold Belt, Mt Isa Inlier. Australian Journal of Earth Sciences 45, 343–361.

Passchier, C.W., Trouw, R.A.J., 1998. Micro-tectonics. Springer-Verlag, Berlin, pp. 1–283.

Passchier, C.W., Trouw, R.A.J., Zwart, H.J., Vissers, R.L.M., 1992. Porphyroblast rotation: eppur si muove? Journal of Metamorphic Geology 10, 283–294.

Pattison, D.R.M., Spear, F.S., Cheney, J.T., 1999. Polymetamorphic origin of muscovite + cordierite + staurolite + biotite assemblages: implications for the metapelitic petrogenetic grid and for P–T paths. Journal of Metamorphic Geology 17, 685–703.

Regnier, J.L., Ring, U., Passchier, C.W., Gessner, K., Gungor, T., 2003.

Contrasting metamorphic evolution of metasedimentary rocks from the Cine and Selimiye nappes in the Anatolide belt, western Turkey. Journal of Metamorphic Geology 21, 699–721.

Reinhardt, J., 1992. Low-pressure, high-temperature metamorphism in a compressional tectonic setting: Mary Kathleen Fold Belt, northeastern Australia. Geological Magazine 129, 41–57.

Rosenfeld, J.L., 1968. Garnet rotation due to the major Paleozoic deformation in southeast Vermont. In: Zen, E-AN, White, W.S., Hadley, J.B. (Eds.), Studies of Appalachian Geology: Northern and Maritime. Interscience publishers, New York, pp. 185–202.

Rubenach, 1992. Proterozoic low-pressure/high temperature metamorphism and an anticlockwise P–T–t path for the Hazeldene area, Mount Isa Inlier, Queensland, Australia. Journal of Metamorphic Geology 10, 333–346.

Rubenach, M.J., Barker, A.J., 1998. Metamorphic and metasomatic evolution of the Snake Creek Anticline, Eastern Succession, Mt Isa Inlier. Australian Journal of Earth Sciences 45, 363–372.

Rubenach, M.J., Lewthwaite, K.A., 2002. Metasomatic albitites and related biotite-rich schists from a low-pressure polymetamorphic terrane, Snake Creek Anticline, Mount Isa Inlier, north-eastern Australia: microstructures and P–T–d paths. Journal of Metamorphic Geology 20, 191–202.

Sayab, M. Decompression through an early clockwise P–T path in the Mt Isa Inlier: implications for early N–S shortening orogenesis. Journal of Metamorphic Geology, in review.

Steinhardt, C., 1989. Lack of porphyroblast rotation in noncoaxially deformed schists from Petrel Cove, South Australia, and its implications. Tectonophysics 158, 127–140.

Thompson, P.H., Bard, J.P., 1982. Isograds and mineral assemblages in the eastern axial zone, Montagne Noire (France). Implications for temperature gradients and P–T history. Canadian Journal of Earth Sciences 19, 129–143.

Turnbull, I.M., 1981. Contortions in the schists of the Cromwell district, Central Otago, New Zealand. New Zealand Journal of Geology and Geophysics 24, 65–86.

Vance, D., Mahar, E., 1998. Pressure–temperature paths from P–T pseudosections and zoned garnets: potential, limitations and examples from the Zanskar Himalaya, NW India. Contributions to Mineralogy and Petrology 132, 225–245.

Whitelock, J., 1989. Structural analysis of the synclinal Scott Outlier, Cattle Creek Area, SSW of Mary Kathleen, Mt Isa Inlier. Unpublished Honors thesis, James Cook University, Townsville, Queensland, pp. 1–301.

Williams, M.L., Jercinovic, M.J., 2002. Microprobe monazite geochronology: putting absolute time into microstructural analysis. Journal of Structural Geology 24, 1013–1028.

Williams, P.F., Jiang, D., 1999. Rotating garnets. Journal of Metamorphic Geology 17, 367–378.